RADIOMETRIC CALIBRATION

VISIBLE/INFRARED IMAGER/RADIOMETER SUITE ALGORITHM THEORETICAL BASIS DOCUMENT

Version 5, Revision 1: May 2002

William P. Byerly
J. Ed Clement
Tim Dorman
Jack Engel
Richard Julian
Shawn W. Miller
James B. Young
Joe A. Walker

RAYTHEON COMPANY
Information Technology and Scientific Services
4400 Forbes Boulevard
Lanham, MD 20706

SRBS Document #: Y3261

SDR: Radiometric Calibration

Doc No: Y3261

Version: 5

Revision: 2

	Function	Name	Signature	Date
Prepared by	SDR Developer	W. BYERLY		5/22/02
Approved by	Relevant IPT Lead	W. BYERLY		5/22/02
Reviewed by	Reviewer	K. JENSEN		5/24/02
Approved by	Chief Scientist	S. MILLER		5/24/02
Released by	Algorithm Lead	P. KEALY		5/24/02

TABLE OF CONTENTS

Page

LIST OF FIGURES

LIST OF TABLES

GLOSSARY OF ACRONYMS

A-D	Analog to Digital
ADC	Analog to Digital Converter
AOI	Angle of Incidence
ARR	Application Related Requirement
ASP	Analog Signal Processor
ATBD	Algorithm Theoretical Basis Document
AVHRR	Advanced Very High Resolution Radiometer
BB	Blackbody
BCS	Blackbody Calibration Source
BMI	Border Match Index
BRDF	Bi-directional Reflectance Distribution Function
BRF	Bi-directional Reflectance Function
CCA	Circuit Card Assembly
CDR	Critical Design Review
CCD	Charge Coupled Device
DC	Digital Count
DCR	DC Restore
DN	Digital Number
DNB	Day/Night Band
DoD	Department of Defense
DPA	Data Processing Architecture
EDR	Environmental Data Record
Ecal	Electronic Calibration
EOS	Earth Observing System
EV	Earth View
FPA	Focal Plane Assembly
GIFOV	Ground Instantaneous Field of View
HAM	Half Angle Mirror
HSI	Horizontal Sampling Interval
HSR	Horizontal Spatial Resolution
IP	Intermediate Product
IPO	Integrated Program Office
LLLS	Low Level Light Sensor
LUT	Lookup Table
MCST	MODIS Characterization Support Team
MODIS	Moderate Resolution Imaging Spectroradiometer
NASA	National Aeronautics and Space Administration
NedT	Noise Equivalent Differential Temperature
NIR	Near Infrared

NIST	National Institute of Standards and Technology
NOAA	National Oceanic and Atmospheric Administration
NPOESS	National Polar-orbiting Operational Environmental Satellite System
NPP	NPOESS Preparatory Project
OBC	Onboard Calibrator
OLS	Operational Linescan System
PDR	Preliminary Design Review
PS	Performance Specification
RCI	Radiometric Correlation Index
RDR	Raw Data Record
RMS	Root Mean Square
ROIC	Read-Out Integrated Circuit
RSB	Reflective Solar Bands
RSR	Relative Spectral Response
RTA	Rotating Telescope Assembly
RVS	Response Versus Scan
SBRS	Santa Barbara Remote Sensing
SCMA	Scattering Measurement Assembly
SD	Solar Diffuser
SDR	Sensor Data Record
SDS	Solar Diffuser Screen
SDSM	Solar Diffuser Stability Monitor
SIS	Spherical Integrating Source
S/MWIR	Short/Mid-Wave Infrared
SNR	Signal-to-Noise Ratio
SRD	Sensor Requirements Document
SV	Space View
SVS	Space View Source
SWIR	Short-Wave Infrared
TDI	Time Delay and Integration
TEB	Thermal Emissive Bands
TIROS	Television Infrared Observation Satellite
TOA	Top of Atmosphere
TP	Technical Publication
TV	Thermal Vacuum
VIIRS	Visible/Infrared Imager/Radiometer Suite
VIS	Visible
VISNIR	Visible/Near Infrared

ABSTRACT

The Visible/Infrared Imager/Radiometer Suite (VIIRS) is scheduled to fly onboard multiple satellites in the National Polar-orbiting Operational Environmental Satellite System (NPOESS). It will produce many science data products, each of which is referred to as an Environmental Data Record (EDR). The VIIRS EDR requirements are described in detail in the *VIIRS Sensor Requirements Document* (SRD). These requirements form the foundation from which both the algorithms and the Sensor are designed and built. A revised version of the SRD was released in November 1999. It included a set of new requirements targeted toward the NPOESS Preparatory Project (NPP); a National Aeronautics and Space Administration (NASA) endeavor to build upon the heritage of the Moderate Resolution Imaging Spectroradiometer (MODIS) beginning in 2005. Incremental updates to the SRD have followed with minor changes. At the time of this writing Version 3, dated June 2000, is the latest issue.

The VIIRS EDR algorithms require radiometric data input from one or more VIIRS spectral bands. These data are ingested in one of three forms:

1) Calibrated Top of Atmosphere (TOA) Radiances
2) Calibrated TOA Reflectances
3) Calibrated TOA Brightness Temperatures

Each of these forms is included in resolution specific Sensor Data Record (SDR) files. The SDR structures are very basic and draw heavily upon heritage for similar Level 1 products.

This document describes the algorithms for converting geolocated digital numbers (i.e. instrument counts) from each verified VIIRS Raw Data Record (RDR) into these SDR products. MODIS emissive band and reflective band Level 1B algorithms provided a baseline for VIIRS. Enhancements to these heritage algorithms were made to accommodate features that are unique to VIIRS, including dual gain bands, the Day/Night Band (DNB), and the along-scan aggregation of sub-pixel detectors as well as to incorporate more rigorous reflective band characterization. These algorithms apply calibration coefficients determined during pre-launch testing and updated as needed to transfer the ground calibration to on-orbit data. Provisions are included to incorporate adjustments into the radiometric calibration to account for instrument temperature, changes in incoming solar flux, and to correct for instrument degradation.

1.0 INTRODUCTION

This Algorithm Theoretical Basis Document (ATBD) describes the algorithm used to produce calibrated top of atmosphere (TOA) radiances, calibrated TOA reflectances, and calibrated TOA brightness temperatures for National Polar-orbiting Operational Environmental Satellite System (NPOESS) Visible/Infrared Imager/Radiometer Suite (VIIRS) sensor data. These are the primary Sensor Data Record (SDR) products of the VIIRS. The calibrated TOA radiance (except Day/Night Band [DNB]) and reflectance products are defined to match the corresponding MODIS Level 1B products (see Section 5.2, reference 3). The DNB calibrated TOA radiances are integrated radiance in W/cm^2-sr whereas the calibrated TOA radiances for the moderate and imagery resolution bands are spectral radiance in W/m^2-sr-micron.

Throughout this document are references to other Raytheon Santa Barbara Remote Sensing (SBRS) documents. These references use the SBRS document number set in italic font and enclosed in brackets (e.g. *[Y12345]*). When a document is first referenced its complete title is given along with the document number.

1.1 PURPOSE AND SCOPE OF DOCUMENT

The main purpose of this ATBD is to establish guidelines for the production of the SDR products. This document describes the required inputs, the theoretical and mathematical description of the retrieval algorithm, practical considerations for implementation, and the assumptions and limitations associated with the products.

This ATBD is part of the VIIRS Algorithm Subsystem's documentation hierarchy as called for in the *VIIRS Software Development Plan [Y2388]*. As shown in Figure 1 the *Performance Specification Algorithm Specification for the VIIRS [PS154640-102]* is the controlling document for this ATBD. The software architecture for implementing the radiometric calibration algorithms is documented in the *VIIRS Build SDR Module Level Software Architecture [Y2479]*.

This document covers the algorithm theoretical basis for the operational retrieval of calibrated TOA radiances, calibrated TOA reflectances, and calibrated TOA brightness temperatures. Any derived products beyond these three SDR products are not discussed beyond brief mention. The geolocation part of the Raw Data Record (RDR) to SDR conversion process is discussed in the *VIIRS Geolocation ATBD [Y3258]*. Information concerning the pre-flight calibration of VIIRS and the transfer of this calibration to on-orbit data is in the *VIIRS Characterization and Calibration Plan [TP 154640-118]*.

This version of the *VIIRS Radiometric Calibration ATBD* is focused on that part of the radiometric calibration that is needed for the near real-time operational conversion of raw instrument counts to calibrated TOA radiances, reflectances, and brightness temperatures. The processing required to derive and update calibration coefficients and correction factors based on the results obtained during the offline analysis of on-orbit calibration mode data is summarized in Section 3.

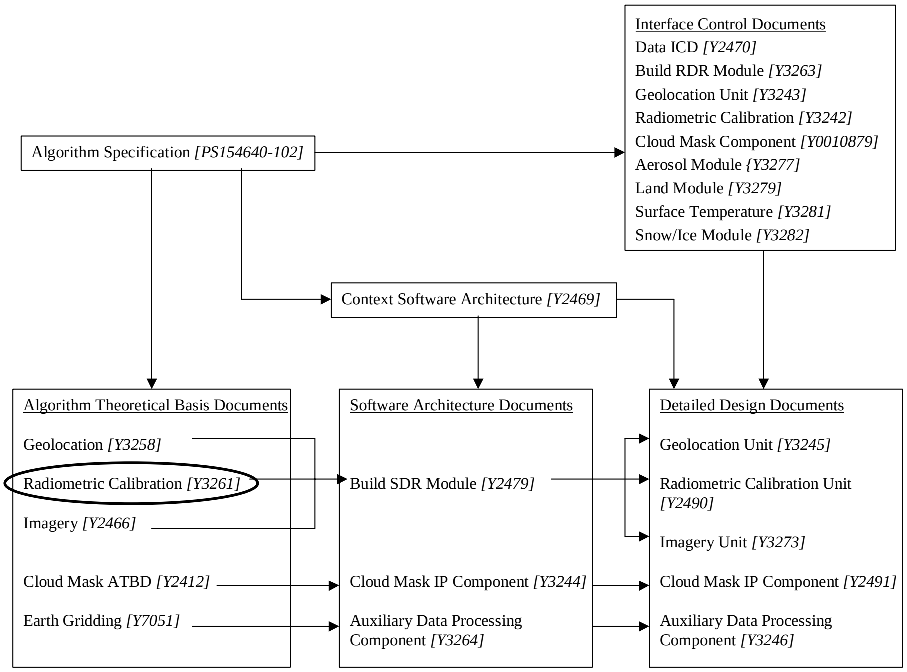

Figure 1. Hierarchy of VIIRS documents that relate to the design of the RDR to SDR S/W. (this ATBD is circled)

The term digital number (DN) is used throughout this document to refer to raw instrument counts. After removal of zero offsets (i.e. the background count that is present when no radiometric signal is present) digital numbers are referred to as “dn”s. Other terminology follows conventions that are in use for MODIS.

1.2 DOCUMENT CONTEXT, CONVENTIONS, AND ORGANIZATION

The organization of this ATBD is to provide introductory information in Section 1. Section 2 provides a brief overview of radiometric calibration including VIIRS instrument characteristics and the radiometric calibration timeline. Section 3 contains the essence of this document—a complete description of the operational radiometric calibration algorithm. Consideration is given to the overall structure, the required inputs, a theoretical description of the products, and practical implementation issues. Section 4 identifies the assumptions and limitations of the radiometric calibration algorithm and Section 5 contains a listing of document references that are cited throughout this document.

Version 5 is the third working version of this document and is a VIIRS Critical Design Review (CDR) deliverable. Revision 1 incorporates corrections, clarifications, and enhancements that were motivated by comments from the CDR. Version 5, Revision 1 is dated May 2002. Changes for Revision 1 include:

- Expanded description of pre-launch calibration and the transfer of pre-launch calibration to on-orbit data
- Addition of a discussion concerning offline processing tasks

- Addition of a description of the VIIRS DC Restore process
- Replaced reflective band algorithm with the methodology to characterize the VIIRS reflective band response function with a second order polynomial
- Expanded discussion concerning cross-VIIRS calibration for terminator orbits
- Revised emissive band algorithm to provide a consistent and complete set of equations
- Expanded Day/Night Band radiometric calibration algorithm
- Addition of a discussion of VIIRS Analog to Digital Converter (ADC) performance

The previous version number (version 4) was issued in May 2001 to address comments received from the VIIRS Preliminary Design Review (PDR). Version 3 was the first version of this ATBD. Its version number was chosen to match the delivery of the previously existing VIIRS EDR ATBDs, which had undergone two previous version releases. Shawn W. Miller and Douglas V. Hoyt authored the Version 3 ATBD (then called *VIIRS RDR to SDR Conversion ATBD*).

2.0 OVERVIEW

2.1 OBJECTIVES OF RADIOMETRIC CALIBRATION

One or more of the SDR products described in this document are necessary inputs to the VIIRS Environmental Data Record (EDR) algorithms. All VIIRS EDR algorithms use these data either directly or indirectly. These SDR products form the link between sensor measurements and algorithm inputs, relating collected photons at the Sensor's aperture to radiance fields at the top of the atmosphere, which in turn are related via the EDR algorithms to surface and/or atmospheric properties.

2.1.1 Requirements Summary

The requirements for the radiometric calibration part of the VIIRS Data Processing Architecture (DPA) are in the *Performance Specification Algorithm Specification for the VIIRS [PS154640-102]*. The DPA is presented in the *VIIRS Context Software Architecture [Y2469]*.

2.1.2 Data Products

The radiometric calibration part of the VIIRS DPA produces the following during operational near real-time processing:

- Sensor Data Record (SDR) files
- Onboard Calibrator Intermediate Product (IP) files
- Calibrated Dual Gain IP files

SDR files contain the calibrated TOA radiances, reflectances, and brightness temperatures as well as geolocation and related information including geodetic latitude and longitude, terrain height, satellite and solar geometry, and (for the Day/Night Band [DNB]) lunar geometry at each VIIRS pixel. The calibrated TOA radiance (except DNB) and calibrated TOA reflectance products are defined to match the corresponding MODIS Level 1B products (see Section 5.2, reference 3). The DNB calibrated TOA radiances are integrated radiance in W/cm^2-sr whereas the calibrated TOA radiances for the moderate and imagery resolution bands are spectral radiance in W/m^2-sr-micron. Details concerning the SDR files are in the *VIIRS Radiometric Calibration Unit Level Detailed Design [Y2490]*.

The Onboard Calibrator IP files contain subsets of each RDR and are the primary input to offline VIIRS performance analysis. Included in these subsets are all raw calibrator view DNs as well as engineering and housekeeping data. Details concerning this IP can also be found in the *VIIRS Radiometric Calibration Unit Level Detailed Design [Y2490]*.

The Calibrated Dual Gain IP files contain unaggregated, calibrated TOA radiances, reflectances, and brightness temperatures for those VIIRS observations that are aggregated along-scan during ground processing into VIIRS pixels prior to storage in the SDR files; i.e. the calibrated dual gain band data from the nadir and near-nadir aggregation zones before aggregation. Details concerning this IP can also be found in the *VIIRS Radiometric Calibration Unit Level Detailed Design [Y2490]*.

2.2 SENSOR OVERVIEW

2.2.1 Sensor Heritage

The VIIRS can be considered as a convergence of three existing sensors; the Operrational Linescan System (OLS), the Advanced Very High Resolution Radiometer (AVHRR), and the Moderate Resolution Imaging Spectroradiometer (MODIS). The OLS and AVHRR have seen extensive operational use. At the time of this writing the MODIS on the *Terra* satellite has been operational for over two years.

The OLS is the operational visible/infrared scanner for the Department of Defense (DoD). Its unique strengths are controlled growth in spatial resolution through rotation of the ground instantaneous field of view (GIFOV) and the existence of a low-level light sensor (LLLS) capable of detecting visible radiation at night. OLS has primarily served as a data source for manual analysis of imagery. The AVHRR is the operational visible/infrared sensor flown on the National Oceanic and Atmospheric Administration (NOAA) Television Infrared Observation Satellite (TIROS-N) series of satellites (Planet, 1988). Its unique strengths are low operational and production cost and the presence of five spectral channels that can be used in a wide number of combinations to produce operational and research products. In December 1999, the National Aeronautics and Space Administration (NASA) launched the Earth Observing System (EOS) morning satellite, *Terra*, which includes the MODIS. This sensor possesses an unprecedented array of thirty-two spectral bands at resolutions ranging from 250 m to 1 km at nadir, allowing for unparalleled accuracy in a wide range of satellite-based environmental measurements.

A VIIRS will be carried aboard each platform of the National Polar-orbiting Operational Environmental Satellite System (NPOESS). NPOESS is a joint mission between DoD, NOAA and NASA. The VIIRS is a single visible/infrared sensor capable of satisfying the needs of all three communities, as well as the general research community. As such, the VIIRS has three key attributes: high spatial resolution with controlled growth off nadir, low production and operational cost, and a large number of spectral bands to satisfy the requirements for generating accurate operational and scientific products.

2.2.2 Spectral Bands

The VIIRS spectral bands as compared to MODIS, OLS, and AVHRR are shown in Table 1. The spectral position of the VIIRS bands is summarized in Figure 2 through Figure 5. The VIIRS moderate and imagery resolution bands are distributed among three focal plane assemblies (FPA). As shown in Figure 6 each moderate resolution band consists of sixteen along-track detectors and each imagery resolution band consists of thirty-two along-track detectors with odd numbered detectors staggered relative to even numbered detectors. The VIIRS Day/Night Band (DNB) is a temperature controlled Charge Coupled Device (CCD) that is mounted near the visible/near-infrared (VisNIR) FPA. The DNB has 672 sub-pixel detectors along-track that are aggregated on board to create sixteen constant 740 m pixels for each along-scan frame.

Table 1. VIIRS spectral bands as compared to other Vis/IR instruments.

VIIRS			MODIS Equivalent			AVHRR-3 Equivalent			OLS Equivalent		
VIIRS Band	Spectral Range (um)	Nadir HSR (m)	Band(s)	Range	HSR	Band	Range	HSR	Band	Range	HSR
DNB	0.500 - 0.900								HRD PMT	0.580 - 0.910 0.510 - 0.860	550 2700
M1	0.402 - 0.422	750	8	0.405 - 0.420	1000						
M2	0.436 - 0.454	750	9	0.438 - 0.448	1000						
M3	0.478 - 0.498	750	3 10	0.459 - 0.479 0.483 - 0.493	500 1000						
M4	0.545 - 0.565	750	4 12	0.545 - 0.565 0.546 - 0.556	500 1000						
I1	0.600 - 0.680	375	1	0.620 - 0.670	250	1	0.572 - 0.703	1100			
M5	0.662 - 0.682	750	13 14	0.662 - 0.672 0.673 - 0.683	1000 1000	1	0.572 - 0.703	1100			
M6	0.739 - 0.754	750	15	0.743 - 0.753	1000						
I2	0.846 - 0.885	375	2	0.841 - 0.876	250	2	0.720 - 1.000	1100			
M7	0.846 - 0.885	750	16	0.862 - 0.877	1000	2	0.720 - 1.000	1100			
M8	1.230 - 1.250	750	5	SAME	500						
M9	1.371 - 1.386	750	26	1.360 - 1.390	1000						
I3	1.580 - 1.640	375	6	1.628 - 1.652	500						
M10	1.580 - 1.640	750	6	1.628 - 1.652	500	3a	SAME	1100			
M11	2.225 - 2.275	750	7	2.105 - 2.155	500						
I4	3.550 - 3.930	375	20	3.660 - 3.840	1000	3b	SAME	1100			
M12	3.660 - 3.840	750	20	SAME	1000	3b	3.550 - 3.930	1100			
M13	3.973 - 4.128	750	21 22 23	3.929 - 3.989 3.929 - 3.989 4.020 - 4.080	1000 1000 1000						
M14	8.400 - 8.700	750	29	SAME	1000						
M15	10.263 - 11.263	750	31	10.780 - 11.280	1000	4	10.300 - 11.300	1100			
I5	10.500 - 12.400	375	31 32	10.780 - 11.280 11.770 - 12.270	1000 1000	4 5	10.300 - 11.300 11.500 - 12.500	1100 1100	HRD	10.300 - 12.900	550
M16	11.538 - 12.488	750	32	11.770 - 12.270	1000	5	11.500 - 12.500	1100			

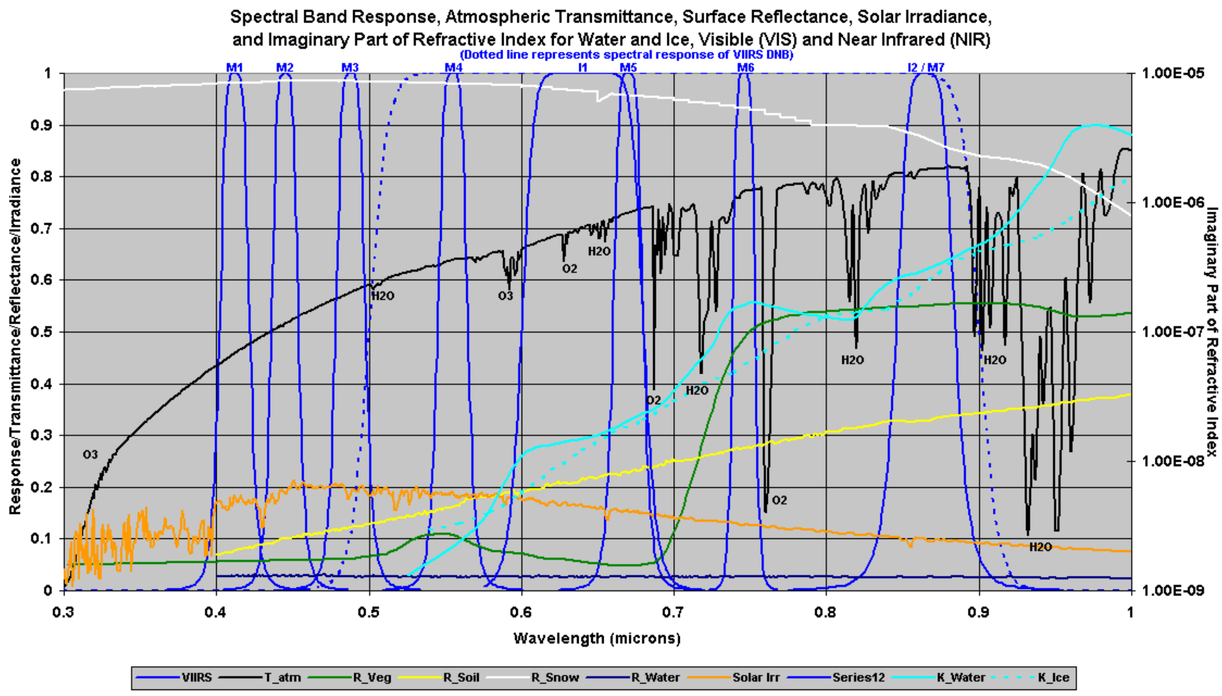

Figure 2. VIIRS spectral bands, visible and near infrared.

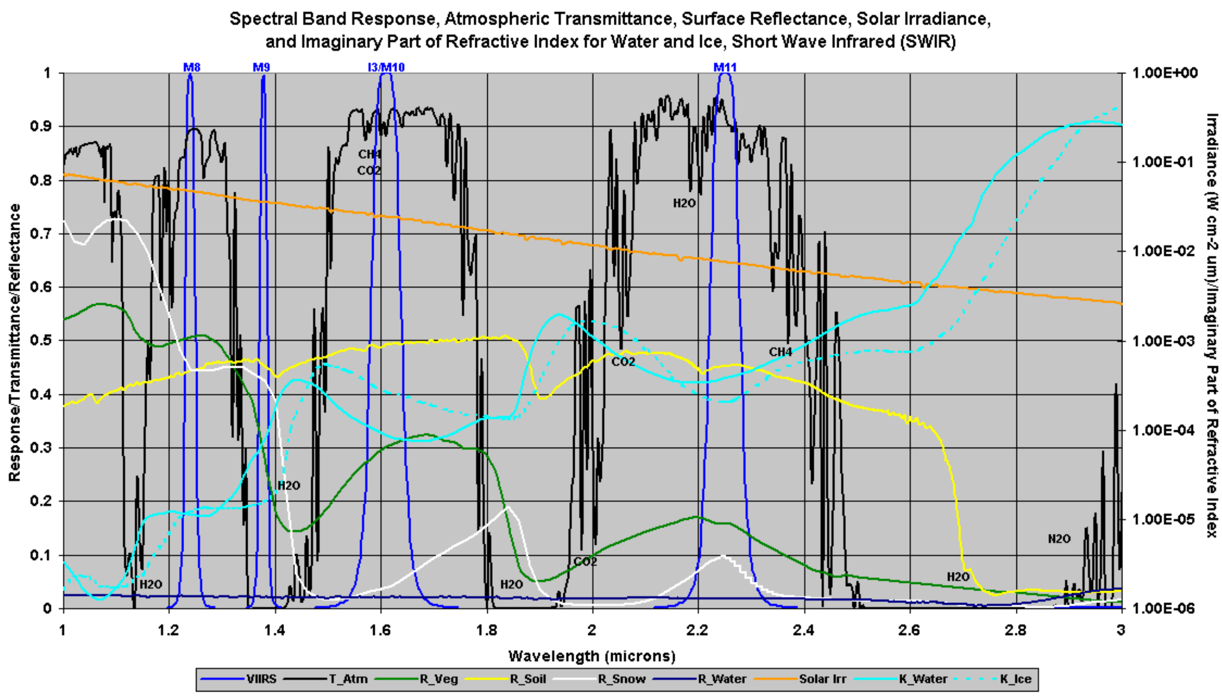

Figure 3. VIIRS spectral bands, shortwave infrared.

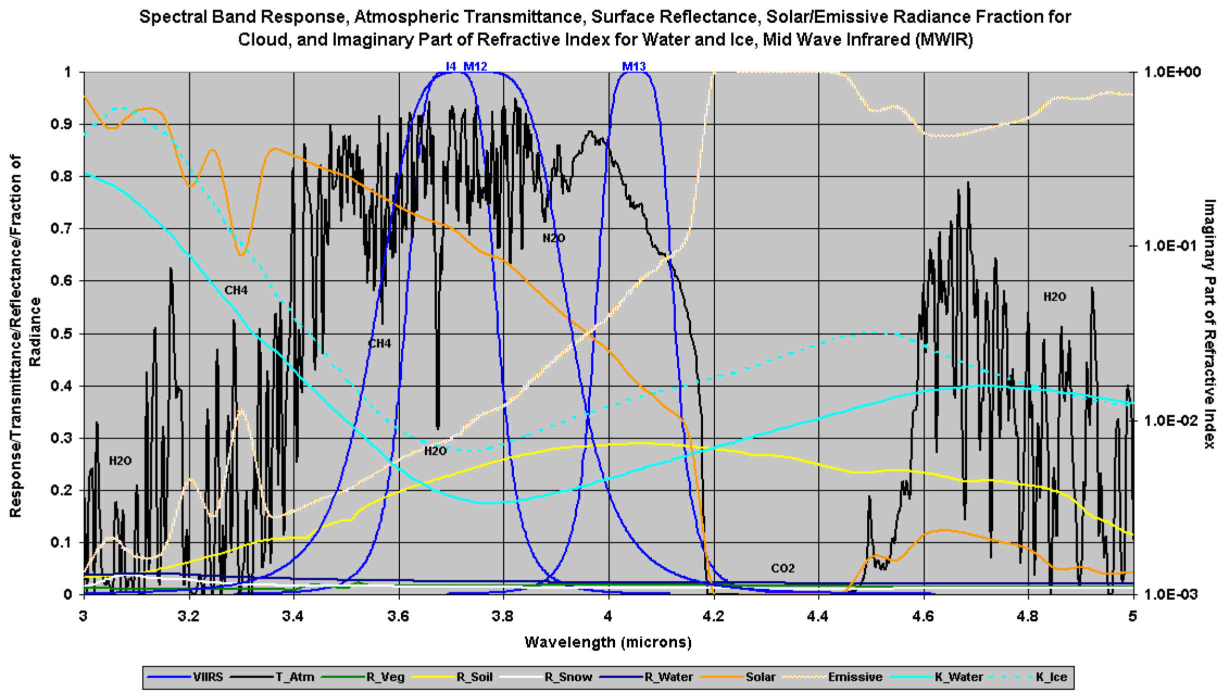

Figure 4. VIIRS spectral bands, midwave infrared.

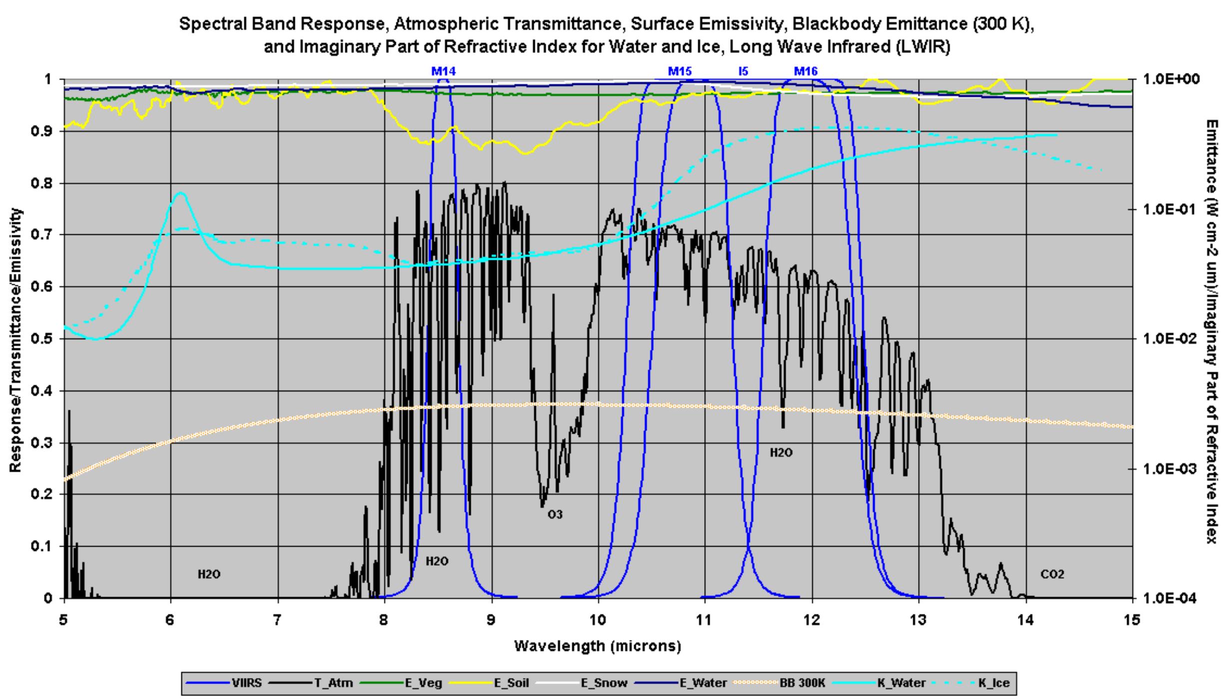

Figure 5. VIIRS spectral bands, longwave infrared.

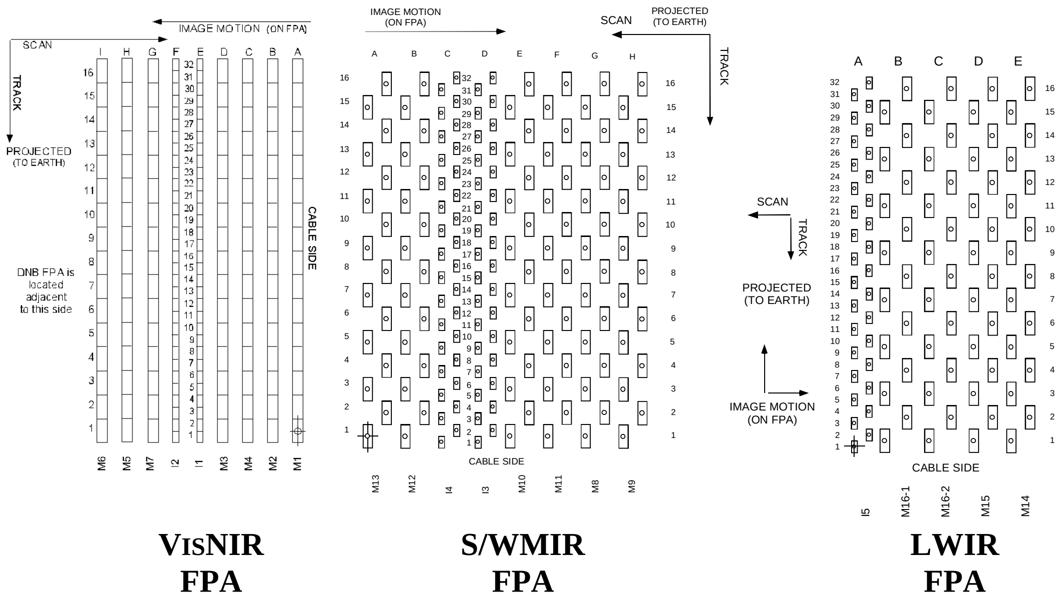

Figure 6. Physical Layout of the Focal Planes.

2.2.3 Sensor Design

Figure 7 illustrates the design concept for the VIIRS, which is designed and built by Raytheon Santa Barbara Remote Sensing (SBRS). At its heart is a Rotating Telescope Assembly (RTA) that minimizes the effects of solar impingement and scattered light and a two-sided Half Angle Mirror (HAM) derotator. Calibration is performed onboard using a solar diffuser for short wavelengths and a V-groove blackbody and deep space view for thermal wavelengths. A Solar Diffuser Stability Monitor (SDSM) is also included to track the performance of the solar diffuser. The nominal altitude for an NPOESS satellite is 833 km. The VIIRS scan extends to 56 degrees on each side of nadir.

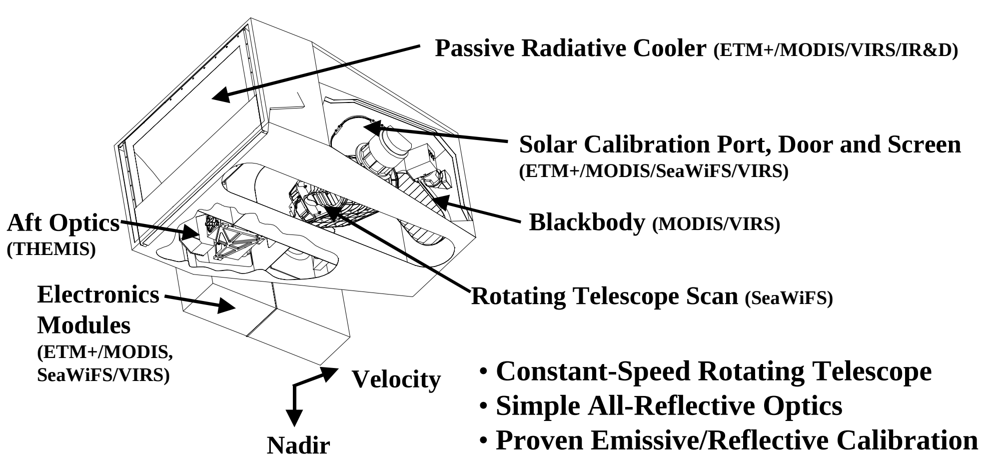

Figure 7. Summary of VIIRS design concepts and heritage.

Figures 8 and 9 present schematic representations of the VIIRS Sensor scan. For most purposes the scan is defined as starting very soon after the HAM turn-around point (Half Angle Mirror Side Change.) This is the point in the scan at which the HAM's angular position becomes perpendicular to the rays from the RTA, and thus the optical signal from the RTA stops falling on one side of the HAM and begins to fall on the other side. From this point, the scan proceeds in a counter-clockwise direction to the space view, through the Earth scan (from night to Sun side), to the blackbody, solar diffuser, and then back to the HAM turn-around point. Thus each scan includes collecting data from each of the calibration sources and the Earth using only one side of the HAM, and each subsequent scan uses alternating sides of the HAM.

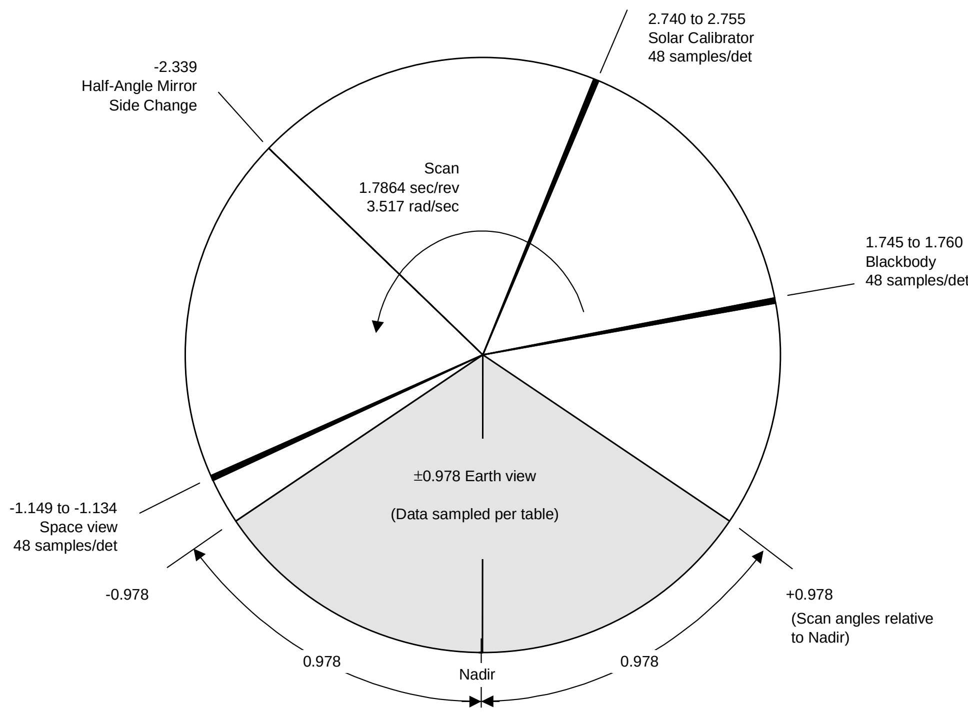

Figure 8. Diagram of VIIRS Scan Pattern

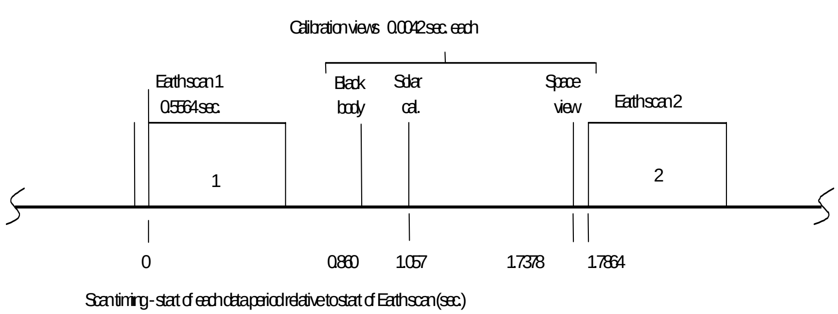

Figure 9. Timeline of typical VIIRS Scan

The *VIIRS Sensor Requirements Document* (SRD) places explicit requirements on spatial resolution for the Imagery EDR. Specifically, the horizontal spatial resolution (HSR) of bands used to meet threshold Imagery EDR requirements must be no greater than 400 m at nadir and 800 m at the edge of the scan. This led to the development of a unique scanning approach which optimizes both spatial resolution and signal-to-noise ratio (SNR) across the scan. The concept is summarized in Figure 10 for the nested imagery resolution bands; the moderate resolution bands follow the same approach at exactly twice the size. The VIIRS moderate and imagery resolution detectors are rectangular, with the smaller dimension projecting along the scan. At nadir, three detector footprints are aggregated to form a single VIIRS "pixel." Moving along the scan away from nadir, the detector footprints become larger both along track and along scan, due to geometric effects and the curvature of the Earth. The effects are much larger along scan. At approximately 32 degrees in scan angle, the aggregation scheme is changed from 3x1 to 2x1. A similar switch from 2x1 to 1x1 aggregation occurs at approximately 45 degrees. The VIIRS scan consequently exhibits a pixel growth factor of only 2 both along track and along scan, compared with a growth factor of 6 along scan which would be realized without the use of the aggregation scheme. Figure 11 illustrates the spatial resolution benefits of the aggregation scheme. The VIIRS Day/Night Band (DNB) is designed with no pixel growth as elements of the DNB CCD array are selected to maintain a constant moderate resolution pixel size across scan.

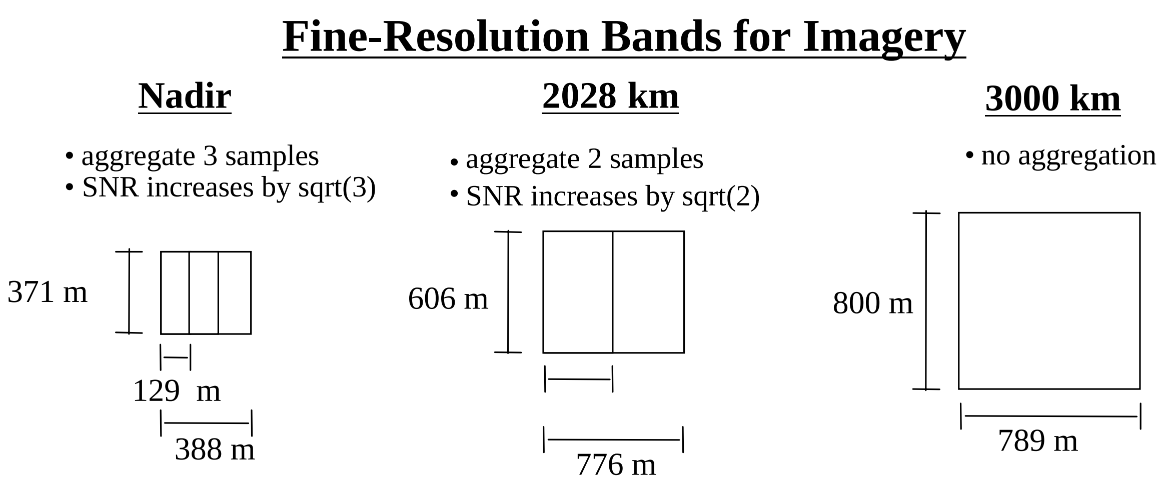

Figure 10. VIIRS detector footprint aggregation scheme for building "pixels." (NOTE: dimensions are approximate)

Some of the VIIRS moderate resolution bands are designed with dual gain in order to cover the required dynamic range within the SNR requirements. The *Closure Memo for PDR Action Items 29, 43, 47, and 78 [Y5563]* demonstrated that there are no effects of gain switching on the calibrated radiance retrieval.

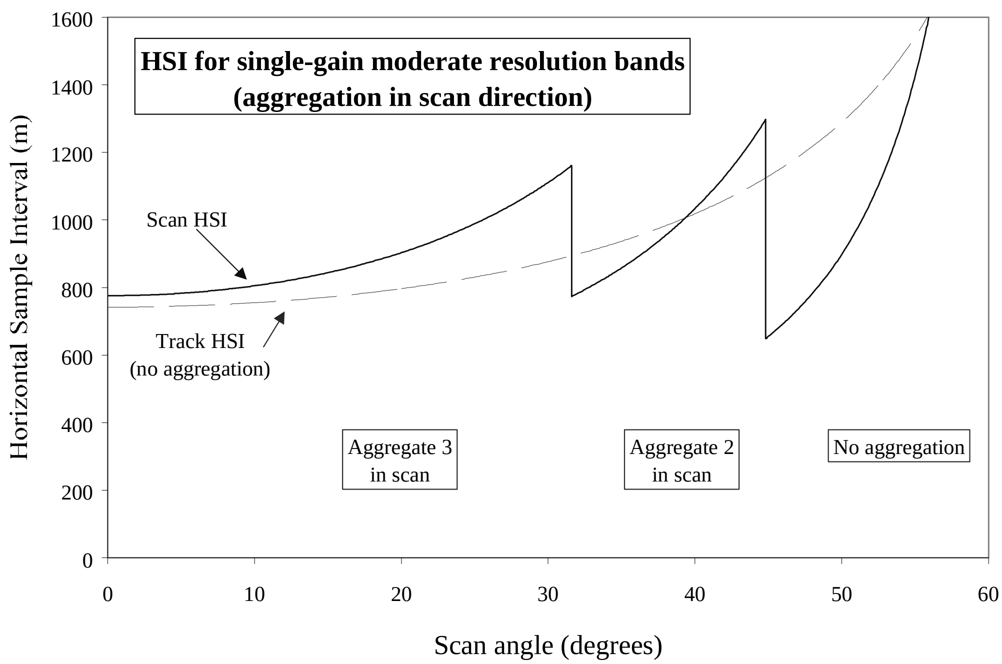

Figure 11. Benefits of VIIRS aggregation scheme in reducing pixel growth at edge of scan.

2.2.4 VIIRS Analog to Digital Converter (ADC) Performance

The performance of the quantizing circuits, or Analog to Digital Converters (ADCs) within VIIRS can have a significant affect on the overall performance of the Sensor, including calibration. Specific areas of concern include integral and differential non-linearity, missing codes, and code patterns (higher and lower than expected frequency or distribution of some ADC outputs.) Additionally, many aspects of the signal processing circuitry can contribute to these types of performance degradations including the analog signal processing circuitry preceding the ADC (gain and offset correction), the ADC itself, and the power, ground and control and data connections to the ADC, to name a few. The design of the VIIRS Analog Signal Processor (ASP) includes provisions to address all of the above concerns in order to ensure that it provides the quality of science data required from the VIIRS Sensor.

The VIIRS ASP design has incorporated many lessons learned from the MODIS program. Specific design considerations include using a 14-bit converter to provide high performance 12-bit data (by truncating the two least significant ADC output bits), operating the Sensor's switching power supplies at a much higher frequency to lower the amount of switching noise present in the power and ground connections to the ADCs during each switching cycle, and synchronizing all converter and digital data transmission processes so that any noise caused by these processes is minimized and consistent during the actual conversion process. In particular, these features of the VIIRS ASP design have been included to avoid the code patterns that are present in some of the MODIS detector channels. These patterns, sometimes referred to as hairy histograms, are believed to be a result of power switching noise that occurs during the sensitive portion of the conversion process and results in some of the least significant output bits being biased towards their low (or high) state. The VIIRS design has addressed this concern by ensuring that the electronic environment of the ADCs is maximally quiet during the conversion process. This design approach was demonstrated prior to PDR using an engineering model system that included a VIIRS ASP card operating in a chassis with a power supply representative of that to be used in the flight Sensor. This engineering model demonstrated the extremely high fidelity desired and with no detectable patterns in the outputs.

2.2.5 VIIRS DC Restore

The Digital Count (DC) restoration process for the VIIRS Sensor is very similar to that employed on the MODIS sensor, but has been modified where necessary to account for differences between the two designs. These differences include the use of dual gain bands[1] and the use of a Rotating Telescope Assembly (RTA) with a dual sided Half Angle Mirror (HAM) derotator in the VIIRS Sensor instead of the simpler single gain band and scan mirror architecture employed in MODIS.

DC Restore (DCR) is used to ensure that the Focal Plane Assembly (FPA) signals digitized by the Sensor's Analog Signal Processor (ASP) are always within the dynamic range of the ASP's Analog to Digital Converters (ADCs). This is done by electronically summing a specific offset onto the FPA output signals for each detector channel such that their minimum, zero scene radiance output is biased to a level corresponding to approximately 200 counts out of the ADCs. This ensures that the lowest level signals from these outputs never drop below the dynamic range of the ADCs, which might otherwise result from aging and radiation effects.

This is a straightforward process for the reflective bands since their zero scene signals are already approximately zero. It is more complicated for the emissive bands since their zero scene radiance output signals are biased on a pedestal resulting from instrument self emission and detector dark current signals. The signal processing circuitry in the VIIRS Sensor is designed to remove the majority of this pedestal by restoring (offsetting) the output signal such that it corresponds to approximately 200 ADC counts when the emissive channels are viewing space.

This process is further complicated since VIIRS determines this offset based on data collected from the on-board blackbody and not the space view. The blackbody view is used for this process in order to avoid signal contamination that would otherwise result when the Moon and/or bright stars are within the space view calibration sector. Though the signals from these objects are mainly of concern to reflective band DC restoration, the architecture of the Sensor requires all bands to be DC restored at the same time. Therefore, the actual offset employed for emissive band DC restoration must be calculated based on the temperature of the blackbody

[1] VIIRS dual gain bands include M1, M2, M3, M4, M5 and M7 on the VisNIR FPA and M13 on the S/MWIR FPA. The dual gain function resides within the Read-Out Integrated Circuit (ROIC) of the FPA and automatically selects between high (default) and low gain based on the input signal level detected during each integration period unless overridden.

and the signal that should result from viewing it. This is done using an on-board look-up table that indicates the expected band output as a function of blackbody temperature, and by having the flight software adjust the offset level based on the difference between the actual and expected outputs.

The HAM introduces two variables that need to be accounted for during DC Restore and/or calibration. First, since the HAM is a two-sided mirror, differences between the reflectance (and emittance) of the two sides need to be tracked. Second, since the angle of incidence (and reflectance) of the source radiance changes as a function of HAM angle, the varying Response Versus Scan (RVS) contribution to overall Sensor transmission (and emission) needs to be taken into account. This latter effect is a significant contributor to calibration, but does not impact DC restoration since the blackbody data used to compute the offset is always collected over a very small angular range centered around the fixed blackbody location.

The scan approach outlined in Section 2.2.3 demonstrates an additional complication with DC restoration. The data for DC restoration are collected towards the middle of each scan, and therefore are not available until after the scan has been completed. This is to ensure that all of the data collected within a scan have been collected with a consistent offset. For calibration purposes this offset, along with biases due to self-emission and dark current, is determined from data collected from the space view at the start of each scan. Therefore it is not necessary to know the actual offset employed for DC restoration (though the offset data is included in the engineering data packets transmitted by the Sensor), but it is important to maintain this same offset throughout the scan.

The two-sided HAM complicates this process since the data for each subsequent scan is collected from alternating sides of the HAM. Therefore, the flight software must keep track of the DC restore offsets calculated from one side of the HAM and save these values for use until that side of the HAM becomes active again. The bookkeeping effort associated with this side tracking and offset application process is described in *Description of DC Restore Process in the VIIRS Sensor [Y0012275]*.

The use of dual gain bands in VIIRS adds one final complication to the DC restore process. It is desirable to collect calibration data for both gain states of the dual gain bands. The dual gain bands normally stay in their high gain modes based on the expected signal levels from the calibration sources. However, the VIIRS Sensor includes the capability to force the dual gain bands into their low gain mode and does so on every other pair of scans[2]. This allows collection of calibration data from both sides of the HAM in both gain modes. This results in an additional number of scans that must be skipped between collection and application of DC restoration data (as indicated in *[Y0012275]*) since the DC restore offsets should be based on

---

[2] M13 low gain supports the Active Fires Application Related Requirement (ARR). Since the low gain signal level from M13 is expected to be on the order of four to eight ADC counts when it is viewing the on-board blackbody it is possible that it will not be forced into low gain mode as indicated in the text. This signal level is too low to be of much use and other methods are being investigated for calibrating this band when it is in the low gain mode.

data collected while the band is in high gain mode. This is not considered a problem since the drift rate for all of the VIIRS bands is expected to be very slow compared to the DC restoration update rate, even for the dual gain bands that need to skip alternating scans.

2.3 RADIOMETRIC CALIBRATION TIMELINE

Radiometric calibration starts early in the VIIRS development and continues through each Sensor's pre-launch testing and mission operations phase.

2.3.1 Pre-Launch

Prior to launch exhaustive tests are performed under ambient and thermal vacuum (TV) conditions to characterize each VIIRS Sensor's performance and to determine its calibration coefficients. Results from these tests provide the initial data that are stored in reflective, emissive, and DNB radiometric calibration lookup tables (LUTs), which are primary inputs to the operational VIIRS radiometric calibration algorithm.

Calibration for the reflective bands is based on TV measurements of illuminated Spherical Integrating Source (SIS) radiance and measurements of the Bi-directional Reflectance Distribution Function (BRDF) of the solar diffuser. Calibration of the emissive bands is based on TV measurements of a Blackbody Calibration Source (BCS). Details concerning these pre-launch tests are in the *VIIRS Characterization and Calibration Plan [TP 154640-118]*. Sections 3.3.1, 3.3.2, and 3.3.3 of this ATBD include summaries of the pre-launch measurements as they pertain to the calibration coefficients used to process on-orbit reflective band, emissive band, and DNB data, respectively.

2.3.2 Early Orbit Activation and Evaluation

During early orbit operations Sensor performance analysis occurs to test the validity of the pre-launch test results to the processing of on-orbit data (see the *VIIRS System Verification and Validation Plan [TP154640-001]*). Adjustments to the reflective, emissive, and DNB radiometric calibration LUTs are made as necessary prior to entering the operational phase. These adjustments are described in Sections 3.3.1, 3.3.2, and 3.3.3.

2.3.3 Operations Phase

During operational VIIRS ground processing radiometric calibration occurs early in the VIIRS data retrieval process; immediately following geolocation of the raw pixel data. The calibrated TOA radiances SDR product (SDR_RAD) is generated for all active bands. The calibrated TOA reflectances SDR product (SDR_REF) is generated for all active reflective bands during day and terminator operations. The calibrated TOA brightness temperatures SDR product (SDR_BT) is generated for all active emissive bands, including three normally reflective bands that are emissive for fires, at all times. Table 2 summarizes the bands for which each product is retrieved.

Table 2. Bands included in the three primary VIIRS SDRs.

Band New (Old)	Center (μm)	SDR_RAD	SDR_REF	SDR_BT	Notes
M1 (Chlor2)	0.412	X	X		Dual Gain
M2 (2)	0.445	X	X		Dual Gain
M3 (Chlor8)	0.488	X	X		Dual Gain
M4 (4)	0.555	X	X		Dual Gain
I1 (5i)	0.645	X	X		Imagery Resolution
M5 (Oc2)	0.672	X	X		Dual Gain
M6 (Oc3)	0.751	X	X		
I2 (6i)	0.865	X	X		Imagery Resolution
M7 (6r)	0.865	X	X	X	Emissive for Fires
M8 (Cloud1)	1.240	X	X	X	Emissive for Fires
M9 (7)	1.378	X	X		
I3 (8i)	1.610	X	X		Imagery Resolution
M10 (8r)	1.610	X	X	X	Emissive for Fires
M11 (9)	2.250	X	X		
M12 (10r)	3.700	X		X	
I4 (10i)	3.740	X		X	Imagery Resolution
M13 (Sst2)	4.050	X		X	Dual Gain
M14 (Sst4)	8.550	X		X	
M15 (11)	10.783	X		X	
I5 (12i)	11.450	X		X	Imagery Resolution
M16 (12r)	12.013	X		X	2 bands in TDI
DNB	0.700	X	X		Day/Night Band

SDRs include quality flags to indicate pixels that contain invalid or questionable data, could not be geolocated, or for which radiometric calibration could not be performed. The *VIIRS Radiometric Calibration Unit Level Detailed Design [Y2490]* contains details concerning the SDR files including these quality flags.

3.0 ALGORITHM DESCRIPTION

3.1 PROCESSING OUTLINE

Radiometric calibration proceeds following the geolocation of VIIRS pixels (see the *VIIRS Build SDR Module Level Software Architecture [Y2479]*). Raw instrument counts (i.e. DN) are scaled and calibration coefficients are applied in accordance with the algorithm presented in Section 3.3. As part of this process the calibration coefficients and correction factors that are read in at run-time from radiometric calibration lookup table (LUT) files are adjusted based on the current on-orbit environment and to account for changes in the Sensor.

3.1.1 Near Real-time Processing

In the context of this ATBD near real-time processing refers to the radiometric calibration that is performed as part of the operational timeline from receipt of downlinked VIIRS RDRs to completion of the corresponding VIIRS EDRs. In general this includes the processing necessary to determine the appropriate zero offsets and correction factor updates to apply to the current Earth view DNs.

3.1.2 Offline Processing

Offline processing includes the processing required to analyze instrument performance, assess Sensor degradation, and adjust the slowly varying calibration coefficients that are read into the radiometric calibration unit during near real-time SDR production. Offline processing includes the processing and analysis of Solar Diffuser (SD) and Solar Diffuser Stability Monitor (SDSM) data that are required to maintain reflective band calibration as well as the following:

- Periodic Onboard Calibrator (OBC) Blackbody (BB) warm-up/cool-down data
- Thermal Emissive Bands (TEB) response and Noise Equivalent Differential Temperature (NedT) trending
- TEB Response Versus Scan (RVS) study with nadir door scanning
- Reflective Solar Bands (RSB) response and Signal-to-Noise Ratio (SNR) trending
- SD and half angle mirror (HAM) degradation analysis
- Lunar data analysis
- Calibration and instrument performance evaluation after configuration change
- Key telemetry points monitoring (BB, instrument, HAM, Focal Plane Assembly [FPA])
- Striping reduction study
- Analog to Digital Conversion (ADC) bit pattern
- Mirror side correlated noise monitoring

3.2 ALGORITHM INPUTS

3.2.1 VIIRS Data

The required inputs for the generation of SDR products are geolocated RDRs, which contain the basic DNs to be converted into calibrated top of atmosphere (TOA) radiances, reflectances, and brightness temperatures as well as engineering data and onboard calibrator view data that are required by the radiometric calibration algorithm. Predetermined calibration coefficients and correction factors are read as lookup tables (LUTs) from Sensor-specific input parameter files.

3.2.2 Non-VIIRS Data

No non-VIIRS data are required for radiometric calibration except for extraterrestrial solar irradiances, which are needed for offline processing of solar diffuser view data. The *VIIRS Data Interface Control Document [Y2470]* describes these data.

3.3 THEORETICAL DESCRIPTION

The MODIS Level 1B documentation (see Section 5.2, references 1, 3, and 5) contains many details about transferring MODIS pre-launch calibration to MODIS on-orbit data. These details include corrections to raw instrument counts to account for non-linearities in analog to digital conversion, detector specific response characteristics, focal plane temperature, and scan angle effects. At the time of this writing the VIIRS has not undergone any of the pre-launch calibration tests that are necessary to define these types of corrections for VIIRS. However it can be anticipated that some of these types of corrections will also be needed for VIIRS. Therefore this version of the *VIIRS Radiometric Calibration ATBD* presents a basic mathematical description of radiometric calibration and recognizes the need to accommodate corrections and adjustments as a practical consideration for the design of the VIIRS radiometric calibration software.

The VIIRS is a conventional differencing radiometer. Instrument background radiation effects are removed by subtracting the cold space view (SV) signal from the Earth view (EV) signal on a scan-by-scan basis. Here scan-by-scan is understood to mean the most recent SV data that has the same HAM side and (in the case of the dual gain bands) the same gain range as the EV observation.

Terminator orbits present a special challenge for the radiometric calibration of VIIRS reflective bands. When in a terminator orbit (i.e. the 17:30 local equator crossing time orbit) the VIIRS solar diffuser is not illuminated by the Sun. A procedure for calibration transfer from non-terminator orbits to terminator orbits is presented in *Terminator Orbit Calibration [Y6875]* and *VIIRS Cross-Calibration Method for Terminator Orbit Sensors [Y0012416]*. This procedure is re-stated in Section 3.3.1.3. Coincident nadir Earth scenes from the 13:30 orbit (which have nearly identical solar zenith angles) are used to adjust the calibration coefficients for the 17:30 orbit.

The signals measured by both the reflective and emissive bands are affected by the reflectance (and emittance) of the Sensor's optical elements. The contribution due to these elements, with the exception the HAM, is constant across the scan angles associated with the Earth and calibration source views. The HAM introduces two variables that need to be accounted for during calibration. First, since the HAM is a two-sided mirror, differences between the reflectance (and emittance) of the two sides need to be tracked. Second, since the angle of incidence (and reflectance) of the source radiance changes as a function of HAM angle, the varying Response Versus Scan (RVS) contribution to overall Sensor transmission (and emission) needs to be taken into account.

Separate algorithms are presented in the following subsections for the VIIRS reflective bands and for the VIIRS emissive bands. Due to its unique design and performance requirements the VIIRS Day/Night Band (DNB) radiometric calibration is treated separately in Section 3.3.3.

3.3.1 Reflective Bands

Reflective VIIRS bands include moderate resolution bands M1 through M11, imagery resolution bands I1, I2, and I3, and the DNB (which is discussed separately in Section 3.3.3). All imagery resolution bands and moderate resolution bands M6, M8, M9, M10 and M11 are single gain. Other moderate resolution reflective bands are dual gain. Calibrated TOA reflectances and calibrated TOA radiances are computed and stored in the SDR files for each reflective band pixel. In addition TOA brightness temperatures are also computed for three reflective bands that are expected to be emissive for fires; i.e. M7, M8, and M10.

An along-scan aggregation is performed following radiometric calibration of the dual gain band DNs as part of the process of building the output SDR products. The aggregation process of dual gain calibrated radiance products exactly matches the aggregation of DNs that is performed on board for the single gain bands. The unaggregated scenes that would otherwise be discarded are saved in an intermediate product file (i.e. the Onboard Calibrator IP) for analysis or production of special interest products that may be desired from time to time.

The equations in this section outline the methodology used to characterize the VIIRS response function over the dynamic range with a second order polynomial. This second order polynomial provides the response function shape and is adjusted to give absolute radiance scale via the use of a one point radiometric calibration. Note that the final nominal VIIRS gain will be adjusted so that the full dynamic range is covered. The nominal final gain setting will provide a VIIRS signal level of approximately 3100 digital counts above the digital count (DC) offset level for the sensor specification levels of maximum radiance, L_{max}.

3.3.1.1 Pre-launch Radiometric Calibration

Pre-launch calibration of the VIIRS reflective bands is accomplished utilizing spectral irradiance lamps and Spectralon panel with calibration traceable to National Institute of Standards and Technology (NIST).

The VIIRS response function is characterized using the macro non-linearity characterization method (i.e. Method 1) as described in *Methodology to characterize VIIRS non-linearity - micro and macro [Y5235]*. Each band, detector channel, and gain state has its own response function.

The equation is:

$$LL = a0 + a1 \cdot dn + a2 \cdot dn^2 \qquad (1)$$

where dn represents the VIIRS signal difference between the SIS and the SVS.

A one point radiometric calibration level is used to determine the spectral radiance scale. The radiometric calibration level has spectral radiance, L_{cal}, and this produces a VIIRS signal, dn_{cal}. The scale factor, F_{scale}, is given by

$$F_{scale} = \frac{L_{cal}}{a0 + a1 \cdot dn_{cal} + a2 \cdot dn_{cal}^2} \qquad (2)$$

The modified polynomial coefficients with proper radiometric scale is given

$$b0 = F_{scale} \cdot a0 \qquad b1 = F_{scale} \cdot a1 \qquad b2 = F_{scale} \cdot a2 \qquad (3)$$

and

$$L = b0 + b1 \cdot dn + b2 \cdot dn^2 \qquad (4)$$

The calibration approach outlined above is to be done in pre-launch thermal vacuum at three instrument temperature plateaus. Thus the coefficient sets are generated for all reflective bands and channels, each gain state (where applicable), and each instrument temperature plateau.

Additional data needed for on-orbit calibration and retrieval include:

1. Solar diffuser Bi-directional Reflectance Distribution Function (BRDF) over the total useful angular and wavelength domain for reflective region, BRDF(ϕ_h, ϕ_v, λ). (Note: angles ϕ_h, ϕ_v are used in the calculation of the solar illumination angle of incidence on the solar diffuser)
2. Solar diffuser screen transmission over the total useful angular domain, $\tau_{sds}(\phi_h, \phi_v)$
3. Relative spectral response, RSR(B, λ)
4. Response versus scan angle, RVS(B, θ)
5. Solar spectral irradiance at Earth orbit, $E_{sun}(\lambda)$
6. Distance from Sun to Earth orbit as a function of time of year, d_{sun_earth}.
7. Angular relationships of solar illumination with respect to spacecraft, sensor to spacecraft, solar diffuser screen, and solar diffuser with respect to sensor.
8. SDSM data including data from attenuated Sun view, solar illuminated solar diffuser, and DC offset level. (These data are used to track changes in the solar diffuser. There are 8 SDSM detector channels that are distributed across the 400 nm to 950 nm spectral region.)
9. Instrument temperature to be used for polynomial coefficient interpolation.

The following sensor and algorithm design elements factor into VIIRS reflective calibration:

1. Each calibration acquisition using the solar diffuser has multiple signal samples (48) per scan line and multiple scan lines (~33). All these data are used to obtain one value of dn that is used in equations (5), (8), (12), and (14).
2. For dual gain bands the calibration data set is split between high and low gain functions.
3. The calibration coefficients employ an interpolation routine if the instrument temperature is different than any of the three instrument temperatures used in the pre-launch thermal vacuum calibration.
4. The reflective region has spectral bands in the visible (VIS), near infrared (NIR) and short-wave infrared (SWIR) regions. The solar diffuser is used for all these bands for on orbit calibration.
5. However, the SDSM tracks solar diffuser BRDF changes for the VIS and NIR regions. The SDSM does not have bands in the SWIR region. An assumption is made (as was done in the MODIS system) that there is no degradation of solar diffuser BRDF in SWIR bands (i.e. M8, M9, M10, M11, and I3).
6. Each SDSM acquired data set has multiple sets of SDSM view of sun (DC_{sun}), solar diffuser (DC_{sd}), and housing (DC_{offset}). The algorithms given in this summary use the effective averaged values - dc_{sun} and dc_{sd} where $dc_{sun} = DC_{sun} - DC_{offset}$ and $dc_{sd} = DC_{sd} - DC_{offset}$. These data are acquired over approximately 33 successive scan lines.
7. There may be minor interpolations of solar diffuser BRDF correction using eight SDSM detector channels and applying them to VIIRS bands M1 through M7 and I1 and I2.

3.3.1.2 On-Orbit Radiometric Calibration

The on-orbit activation phase involves adjusting the pre-launch calibration coefficients. This is done for both spectral radiance and reflectance domains. The solar illuminated solar diffuser serves as the calibration source.

$$F_{initial\_on\_orbit} = F_{i=0} = \frac{\dfrac{\int RVS(\theta_{sd}) \cdot \tau_{sds}\left(\phi h_{i=0}, \phi v_{i=0}\right) \cdot RSR(\lambda) \cdot E_{sun}(\lambda) \cdot \cos\left(\phi_{sun\_sd}\right) \cdot BRDF_{sd}\left(\phi h_{i=0}, \phi v_{i=0}\right) \, d\lambda}{\int RSR(\lambda) \, d\lambda}}{\left(b0 + b1 \cdot dn_{initial\_on\_orbit} + b2 \cdot dn_{initial\_on\_orbit}{}^{2}\right)} \tag{5}$$

In the spectral radiance domain the initial modified polynomial coefficients are given by.

$$c0_{i=0} = F_{initial\_on\_orbit} \cdot b0 = F_{i=0} \cdot b0$$

$$c1_{i=0} = F_{initial\_on\_orbit} \cdot b1 = F_{i=0} \cdot b1$$

$$c2_{i=0} = F_{initial\_on\_orbit} \cdot b2 = F_{i=0} \cdot b2 \tag{6}$$

The resultant earth view (ev) spectral radiance retrieval algorithm is

$$L_{ev}(\theta_{ev}) = \frac{1}{RVS(\theta_{ev})} \cdot \left(c0_{i=0} + c1_{i=0} \cdot dn_{ev} + c2_{i=0} \cdot dn_{ev}^{\,2} \right) \tag{7}$$

Equations (5), (6), and (7) address only the initial on-orbit update of the reflective band spectral radiance calibration coefficients and assume pre-launch characterization of the solar diffuser BRDF. Subsequent updates use the SDSM tracking capability, which tracks changes in the solar diffuser BRDF. The associated correction factor assumes that the solar diffuser screen (SDS) has been characterized pre-launch and that this function does not change on orbit. Here the index i=0 corresponds to the initial on-orbit update. Subsequent updates will be i=1, 2, 3 ... Using this approach:

$$F_i = \frac{\dfrac{\displaystyle\int RVS(\theta_{sd}) \cdot \tau_{sds}\left(\phi_{h_i}, \phi_{v_i}\right) \cdot RSR(\lambda) \cdot E_{sun}(\lambda) \cdot \cos(\phi_{sun\_sd}) \cdot BRDF_{sd}\left(\phi_{h_i}, \phi_{v_i}\right) d\lambda}{\displaystyle\int RSR(\lambda)\, d\lambda}}{\left[c0_{i-1} + c1_{i-1} \cdot dn_i + c2_{i-1} \cdot (dn_i)^2 \right]} \tag{8}$$

In the spectral radiance domain the modified polynomial coefficients are given by:

$$c0_i = F_i \cdot c0_{i-1} \qquad c1_i = F_i \cdot c1_{i-1} \qquad c2_i = F_i \cdot c2_{i-1} \tag{9}$$

The resultant earth view (ev) spectral radiance retrieval algorithm is:

$$L_{ev}(\theta_{ev}) = \frac{1}{RVS(\theta_{ev})} \cdot \left(c0_i + c1_i \cdot dn_{ev} + c2_i \cdot dn_{ev}^{\,2} \right) \tag{10}$$

The Solar Diffuser Stability Monitor (SDSM) is used to track changes in solar diffuser BRDF. In an analogous manner that "dn" represents the VIIRS signal difference between scene/calibration signal and space view; "dc" represents an equivalent digital count obtained by taking the SDSM detector channel signal difference between Sun/solar diffuser and the offset level. The updated solar diffuser BRDF used in equation (8) is given in equation (11).

$$BRDF\left(\phi_{h_i}, \phi_{v_i}\right) = \frac{\dfrac{dc_{sd}\left(\phi_{h_i}, \phi_{v_i}\right)}{dc_{sd}\left(\phi_{h_{i-1}}, \phi_{v_{i-1}}\right)} \cdot \dfrac{\tau_{sds}\left(\phi_{h_{i-1}}, \phi_{v_{i-1}}\right)}{\tau_{sds}\left(\phi_{h_i}, \phi_{v_i}\right)}}{\dfrac{dc_{sun_i}}{dc_{sun_{i-1}}} \cdot \left(\dfrac{d_{sun\_earth_{i-1}}}{d_{sun\_earth_i}} \right)^2} \cdot BRDF\left(\phi_{h_{i-1}}, \phi_{v_{i-1}}\right) \tag{11}$$

The corresponding equations associated with spectral reflectance (BRDF) are:

$$G_{initial\_on\_orbit} = G_{i=0} = \frac{\dfrac{\int RVS(\theta_{sd})\cdot\tau_{sds}\left(\phi_{h_{i=0}},\phi_{v_{i=0}}\right)\cdot RSR(\lambda)\cdot E_{sun}(\lambda)\cdot\cos\left(\phi_{sun\_sd}\right)\cdot BRDF_{sd}\left(\phi_{h_{i=0}},\phi_{v_{i=0}}\right)\,d\lambda}{\int RSR(\lambda)\cdot E_{sun}(\lambda)\cdot\cos\left(\phi_{sun\_sd}\right)\,d\lambda}}{\left(b0 + b1\cdot dn_{initial\_on\_orbit} + b2\cdot dn_{initial\_on\_orbit}^{\;2}\right)} \qquad (12)$$

In the spectral reflectance (BRDF) domain the initial on orbit modified polynomial coefficients are given by:

$$d0_{i=0} = G_{initial\_on\_orbit}\cdot b0 = G_{i=0}\cdot b0$$

$$d1_{i=0} = G_{initial\_on\_orbit}\cdot b1 = G_{i=0}\cdot b1$$

$$d2_{i=0} = G_{initial\_on\_orbit}\cdot b2 = G_{i=0}\cdot b2 \qquad (13)$$

The resultant Earth view (ev) spectral reflectance retrieval algorithm is:

$$BRDF_{ev}\left(\theta_{ev}\right) = \frac{1}{RVS\left(\theta_{ev}\right)\cdot\cos\left(\phi_{sun\_earth}\right)}\cdot\left(d0_{i=0} + d1_{i=0}\cdot dn_{ev} + d2_{i=0}\cdot dn_{ev}^{\;2}\right) \qquad (14)$$

Equations (12), (13), and (14) address only the initial on-orbit update of the reflective band reflectance calibration coefficients and assume pre-launch characterization of the solar diffuser BRDF. Subsequent updates use the SDSM tracking capability, which tracks changes in the solar diffuser BRDF. The associated correction factor assumes that the solar diffuser screen (SDS) has been characterized pre-launch and that this function does not change on orbit. Note: index i=0 corresponds to the initial on-orbit update. Subsequent updates will be i=1, 2, 3 ... Using this approach:

$$G_i = \frac{\dfrac{\int RVS(\theta_{sd})\cdot\tau_{sds}\left(\phi_{h_i},\phi_{v_i}\right)\cdot RSR(\lambda)\cdot E_{sun}(\lambda)\cdot\cos\left(\phi_{sun\_sd}\right)\cdot BRDF_{sd}\left(\phi_{h_i},\phi_{v_i}\right)\,d\lambda}{\int RSR(\lambda)\cdot E_{sun}(\lambda)\cdot\cos\left(\phi_{sun\_sd}\right)\,d\lambda}}{\left[d0_{i-1} + d1_{i-1}\cdot dn_i + d2_{i-1}\cdot\left(dn_i\right)^2\right]} \qquad (15)$$

In the spectral reflectance (BRDF) domain updated on orbit polynomial coefficients are given by:

$$d0_i = G_i \cdot d0_{i-1} \qquad d1_i = G_i \cdot d1_{i-1} \qquad d2_i = G_i \cdot d2_{i-1} \tag{16}$$

The resultant Earth view (ev) spectral reflectance retrieval algorithm is:

$$BRDF_{ev}(\theta_{ev}) = \frac{1}{RVS(\theta_{ev}) \cdot \cos(\phi_{sun\_earth})} \cdot \left(d0_i + d1_i \cdot dn_{ev} + d2_i \cdot dn_{ev}^{\ 2} \right) \tag{17}$$

In the case of the dual gain reflective bands the on-board calibrator sources are viewed with alternating gain ranges so that a complete set of gain range-HAM side combinations is acquired every four scans. The radiometric calibration algorithm selects the appropriate scan's calibrator view data to use when processing a scan by selecting from the most recent data that was taken with the same gain range and HAM side as that of the Earth view scene being processed.

Gain specific correction and conversion factors are stored as LUTs for use with the dual gain reflective bands. This adds a dimension to each factor and introduces the requirement on the processing software to identify and select the correct values to use for each sample.

Following radiometric calibration of each dual gain DN an along-scan aggregation is performed as part of the process of building the output SDR products. This aggregation is performed to exactly match the aggregation that is performed on board for the single gain bands. Calibrated TOA reflectances and TOA radiances for the unaggregated sub-pixel samples that would otherwise be discarded are saved in the Calibrated Dual Gain IP file for analysis or production of special interest products that may be desired from time to time. The Calibrated Dual Gain IP file is described in detail in the *VIIRS Radiometric Calibration Unit Level Detailed Design [Y2490]*.

3.3.1.3 Terminator Orbits

The VIIRS is designed to operate in any orbit. However, one of the key design features includes an internal solar diffuser that cannot be illuminated by the Sun when the Sensor is flying in a terminator (i.e. 17:30) orbit. Therefore, the method for calibrating the reflective bands on a Sensor in a terminator orbit is to transfer the calibration from one of the well-calibrated midday (non-terminator) orbiting Sensors. Earth targets are used in this approach.

Such cross-calibration has been done successfully in the past (see Section 5.2, references 2, 4, 8, 9, and 10). In fact VIIRS has advantages over those past successes. The Sensors are "identical," so the errors associated with spectral interpolation and footprint matching are greatly reduced. The cross-calibration can also be done using nadir-view scenes, so that errors associated with Bi-directional Reflectance Function (BRF) variations are also reduced. The remaining major error term, mis-registration of the scene, should also be reduced since it is not necessary to aggregate pixels to perform GIFOV matching as is necessary with sensors having different footprints.

Scene selection is important in reducing cross-calibration errors. Of course the scenes must overlap. Furthermore, good scenes possess the following characteristics:

1) High reflectance (greater than about 0.3)
2) Spatial uniformity

3) Spectral uniformity
4) Temporal invariance of reflectance
5) Little or no vegetation
6) "Near" Lambertian surface
7) Adequate size for averaging
8) Infrequent rainy and/or cloudy conditions

Saturated pixels are ignored during cross-calibration. Pixels may also be eliminated if surrounding pixels have significant variation from the central pixel.

Scene registration has been a significant effort in prior cross-calibrations. Since the scenes are acquired by two VIIRS sensors that have different track directions, the scenes must be rotated and registered. Registration is done using some sort of ground control points (GCPs), such as roads, shorelines, feature edges, or the like. Calibration errors are relatively insensitive to rotation errors. Che (see Section 5.2, reference 2) found only 1% error for a 20 degree rotation and 1.5% for a 40 degree rotation. Evaluation of scene registration quality may be achieved by using two merit functions, the Border Match Index (BMI) and the Radiometric Correlation Index (RCI) (see Section 5.2, reference 2). Optimization of scene matching is done by maximizing the product of BMI and RCI. When the product of these two is near 0.9, a good scene match is indicated.

The sub-satellite points for the 13:30 and 17:30 VIIRS orbits cross paths. Crossings occur each day separated by about 2 hours and 20 minutes (i.e., 140 minutes) and by about 39 minutes such that both satellites have the same nadir view of the same site on the Earth. These crossings occur in the polar regions. Around the equinoxes, the Sun is too close to the horizon to provide any opportunities for calibration, leading to gaps of about 80 days twice each year.

The calibration of the 17:30 VIIRS Sensor can be expected to proceed as follows:

1. The reflectance is measured using the two VIIRS Sensors in 13:30 and 17:30 orbits, both of which are looking at the nadir and both of which have nearly the same solar zenith angles. (The solar azimuth angles differ by about 34 degrees.)
2. The measured ratio of these reflectances is then calculated.
3. The theoretical ratio is calculated using measured or assumed values for surface reflectance and aerosol optical thickness.
4. The measured ratio is adjusted to match the theoretical ratio by adjusting the gain of the 17:30 VIIRS.
5. The theoretical ratio is not exact, but has some error in it caused by uncertainties in the surface reflectance, aerosol optical thickness, and so forth. These error sources are quantified below.

Errors in calibration are expected to be between 4 and 5% for RSBs in the 17:30 VIIRS orbit. This is within the stated calibration accuracy of 5% for terminator orbit Sensors. For the M4 band, the following list summarizes the contributions to systematic error in the calculation of the reflectances for the Sensor in the 17:30 orbit.

1. For an uncertainty in aerosol optical thickness of 0.03 (SRD threshold), the uncertainty in the reflectance ratio is 0.44%.
2. For an uncertainty in surface reflectance of 0.05 (SRD threshold), the reflectance ratio uncertainty is 0.36%. The nadir points are in polar regions so the surface reflectances are of the order of 60-70% in the simulations.
3. The major source in uncertainty of surface reflectance arises from the choice of the surface BRDF. An estimation of this term results from the comparison of a Lambertian surface to a surface using Roujean's BRDF set equal to a surface consisting of evenly spaced hillocks whose height is equal to one tenth of their spacing. Because this surface casts shadows, it has a different response to solar zenith and azimuth angles compared to a Lambertian surface. The maximum observed difference in ratio of 17:30 to 13:30 orbits is 3.6%. Assuming that these two types of surfaces bracket the real BRDF, the uncertainty arising from the choice of BRDF is about 1.8%.
4. The systematic error arising from uncertainties in solar zenith angle is taken to be negligible since the solar zenith angles themselves are well known.
5. Striping or fixed pattern noise is expected to be small after sufficient sampling has been made and histogram equalization has been applied. It is taken to be 0.1%.
6. Ground sample orientation including slope of the surface and location offset errors are expected to be small and are estimated at 0.2%.
7. Errors in water vapor amount and ozone amount are expected to be negligible because water does affect the band and ozone concentrations are relatively stable over 140 minutes.
8. Sub-pixel clouds may occur but can probably be eliminated as outliers.
9. The traceability to NIST for the 13:30 VIIRS is 2%.

The error for the M1 band is smaller than for the M4 band because Rayleigh scattering is greater and the relative contributions, and hence uncertainties, from the surface reflectance and aerosol optical thickness are less.

3.3.2 Emissive Bands

The VIIRS emissive bands are the moderate resolution bands M12 through M16 and the imagery resolution bands I4 and I5. Calibrated TOA radiances and calibrated TOA brightness temperatures are computed and stored in resolution specific SDR files for each of these emissive band's pixels.

An along-scan aggregation is performed following radiometric calibration of the M13 DNs as part of the process of building the output SDR products. This aggregation of calibrated radiance products exactly matches the aggregation of DN that is performed on board for the single gain bands. The unaggregated scenes that would otherwise be discarded are saved in an intermediate product file (i.e. the Onboard Calibrator IP) for analysis or production of special interest products that may be desired from time to time.

3.3.2.1 Pre-launch Radiometric Calibration

During thermal vacuum calibration, the spectral radiance from the Blackbody Calibration Source (BCS) is given by

$$L_{BCS\_PATH} = RVS_{BCS}\, \varepsilon_{BCS}\, L(T_{BCS}) + (1 - RVS_{BCS})L(T_{HAM}) + L_{BKG} \tag{18}$$

where RVS_{BCS} is the Response Versus Scan at the angle of incidence (AOI) for the BCS (RVS_{BCS} is nothing more than a weighting factor due to the variation in reflectance of the HAM as a function of scan angle), ε_{BCS} represents the BCS emittance, $L\{T_{BCS})$ is the radiance calculated from the Planck equation at the BCS temperature T_{BCS}, $L(T_{HAM}\}$ is the radiance calculated from the Planck equation at the half angle mirror (HAM) temperature, and L_{BKG} is the instrument background radiance exclusive of the HAM's RVS variation. The second term of this equation represents the emission from the HAM. This term is separated from the total instrument background to explicitly capture its scan angle and temperature dependence. The BCS is temperature cycled over an interval of 190-340 K.

Similarly, when the VIIRS views the Space View Source (SVS), the spectral radiance of SVS path is given by

$$L_{SVS\_PATH} = RVS_{SVS}\, \varepsilon_{SVS}\, L(T_{SVS}) + (l - RVS_{SVS})\, L(T_{HAM}) + L_{BKG}$$

$$= (l - RVS_{SVS})\, L(T_{HAM}) + L_{BKG} \tag{19}$$

since $L(T_{SVS})$ is essentially = 0

To remove the variable instrument background effect, the SVS term is subtracted from the input signal. Thus, the spectral radiance difference is

$$\Delta L_{BCS} = L_{BCS\_PATH} - L_{SVS\_PATH} = RVS_{BCS}\, \varepsilon_{BCS}\, L(T_{BCS}) + (RVS_{SVS} - RVS_{BCS})L(T_{HAM}) \tag{20}$$

RVS_{BCS} and RVS_{SVS} are HAM side and spectral band dependent. RVS is not expected to vary from detector to detector within the same spectral band.

For a specific VIIRS thermal emissive band (B), the band-averaged radiance difference, due to the BCS path and the SVS path, is

$$\Delta L_{BCS}(B) = RVS_{BCS}\varepsilon_{BCS}\overrightarrow{L(T_{BCS})} + (RVS_{SVS} - RVS_{BCS})\overrightarrow{L(T_{HAM})} \; . \tag{21}$$[3]

where

[3] Mathcad was used to write some of the equations. The arrow over some parameters indicates a mean.

$$\overrightarrow{L(T_{BCS}, B)} = \frac{\int L(T_{BCS}, \lambda_B) RSR(B, \lambda_B)\, d\lambda}{\int RSR(B, \lambda_B)\, d\lambda} \tag{22}$$

and RSR(B, λ_B) represents the wavelength-dependent Relative Spectral Response (normalized to unity at peak) for band B as determined by pre-launch testing. A similar expression for the band integration applies to the second term on the right-hand side of equation (21). Note that throughout this discussion, the channel number indexes are suppressed for clarity.

The band-integrated radiance difference $\Delta L_{BCS}(B)$ is a function of $DN_{BCS} - DN_{SVS}$. Let

$$dn_{BCS} = \frac{1}{N_{scans}} \cdot \sum_{n=1}^{N_{scans}} \left(\frac{1}{M_{BCS}} \cdot \sum_{m=1}^{M_{BCS}} DN_{BCS} - \frac{1}{M_{SVS}} \cdot \sum_{m=1}^{M_{SVS}} DN_{SVS} \right) \tag{23}$$

where M_{BCS} (number of BCS frames), M_{SVS} (number of SVS frames), and N_{scans} (number of scans) are appropriate averaging samples to optimize the calibration coefficients.

On the basis of experience with similar instruments and observed temperature dependencies, a temperature-dependent second-order nonlinear behavior for $\Delta L_{BCS}(B,T_{inst})$ is postulated.

$$\Delta L_{BCS}(B,T_{inst}) = a_{0\_BCS}(B,T_{inst}) + a_{1\_BCS}(B,T_{inst}) * dn_{BCS} + a_{2\_BCS}(B,T_{inst}) * (dn_{BCS})^2 \tag{24}$$

or

$$RVS_{BCS}\varepsilon_{BCS}\overrightarrow{L(T_{BCS})} + (RVS_{SVS} - RVS_{BCS})\overrightarrow{L(T_{HAM})} \;.$$

$$= a_{0\_BCS}(B,T_{inst}) + a_{1\_BCS}(B,T_{inst}) * dn_{BCS} + a_{2\_BCS}(B,T_{inst}) * (dn_{BCS})^2 \tag{25}$$

The BCS calibration coefficients $a_{0\_BCS}(B,T_{inst})$, $a_{1\_BCS}(B,T_{inst})$, and $a_{2\_BCS}(B,T_{inst})$ are determined by least-squares fitting to the corresponding data. In this formulation, the $a_{0\_BCS}(B,T_{inst})$ term is viewed as part of the least-squares fitting process. It is expected to take on small nonzero values. The contribution from the nonlinear response term $a_{2\_BCS}(B,T_{inst})$ is very small compared to the linear response term. Apart from the temperature-dependent behavior, both $a_{0\_BCS}(B,T_{inst})$ and $a_{2\_BCS}(B,T_{inst})$ terms are fixed for the on-orbit operation.

3.3.2.2 On-Orbit Radiometric Calibration

When the VIIRS views the Onboard Calibrator (OBC) Blackbody (BB), the spectral radiance after the HAM includes the OBC BB emitted radiance reflected by the HAM, the HAM emittance, the cavity contributors reflected by the OBC BB and then in turn by the HAM, and the remaining instrument background radiance. Thus

$$L_{OBC\_PATH} = \varepsilon_{OBC}L(T_{OBC})RVS_{OBC} + (1 - RVS_{OBC})L(T_{HAM}) + (1-\varepsilon_{OBC})\,[F_{sh}L(T_{sh},\lambda_B)+ F_{cav}L(T_{cav},\lambda_B) + F_{tele}L(T_{tele},\lambda_B)]RVS_{OBC} + L_{BKG} \quad (26)$$

where ε_{OBC} is the OBC BB emittance, $(1 - \varepsilon_{OBC})$ is the reflectance of the OBC BB, and $(1 - \varepsilon_{OBC})[F_{sh}L(T_{sh},\lambda_B)+ F_{cav}L(T_{cav},\lambda_B) + F_{tele}L(T_{tele},\lambda_B)]$ is a OBC BB reflectance correction term. RVS_{OBC} is HAM side and spectral band dependent. RVS is not expected to vary from detector to detector within the same spectral band.

T_{sh} and T_{cav} is obtained from thermistor data using fifth order polynomials that may be implemented as lookup tables. T_{HAM} and T_{tele} are from thermistors that may not be mounted on the rotating parts.

The terms F_{sh}, F_{cav}, and F_{tele} are weighting factors that represent the share of the reflectance correction that derive from the OBC BB shield, the cavity (between OBC shield and telescope), and the telescope respectively. These weighting factors are determined pre-launch. Their values are geometrical factors and are assumed to be constant on orbit.

From equations (19) and (26), the spectral radiance difference attributed to the OBC BB path and the space view (SV) path is given by

$$\Delta L_{OBC} = L_{OBC\text{-}PATH} - L_{SV\_PATH}$$

$$= RVS_{OBC}\varepsilon_{OBC}L(T_{OBC}) + (RVS_{SV} - RVS_{OBC})L(T_{HAM}) + RVS_{OBC}(1-\varepsilon_{OBC})[F_{sh}L(T_{sh},\lambda_B) + F_{cav}L(T_{cav},\lambda_B) + F_{tele}L(T_{tele},\lambda_B)] \quad (27)$$

For a specific VIIRS band, the band-averaged radiance difference between the OBC BB path and the space view path is given by

$$\Delta L_{OBC}(B) = RVS_{OBC}\,\varepsilon_{OBC}\cdot\overrightarrow{L(T_{OBC})} + (RVS_{SV} - RVS_{OBC})\cdot\overrightarrow{L(T_{HAM})} \ldots + (1-\varepsilon_{OBC})\cdot RVS_{OBC}\left(F_{sh}\cdot\overrightarrow{L(T_{sh})} + F_{cav}\cdot\overrightarrow{L(T_{cav})} + F_{tele}\cdot\overrightarrow{L(T_{tele})}\right) \quad (28)$$

where $\overrightarrow{L(T_{OBC})}$, $\overrightarrow{L(T_{HAM})}$, $\overrightarrow{L(T_{sh})}$, $\overrightarrow{L(T_{cav})}$, and $\overrightarrow{L(T_{tele})}$ are the Planck emission terms determined using equation (22). T_{OBC} data comes from thermistor temperature sensors. In order to obtain very low uncertainty a three component natural log equation is used.

Earth view (EV) sector radiances (except from the low gain M13 band) are determined using the on-orbit calibration linear coefficient obtained with the OBC BB and the space view, and the pre-launch offset and second-order calibration coefficients determined from the thermal vacuum BCS data sets. Equation (29) describes the use of these coefficients

$$\Delta L_{EV}(B,T_{inst}) = a_{0\_BCS}(B,T_{inst}) + b_{1\_OBC}(B,T_{inst})*dn_{EV} + a_{2\_BCS}(B,T_{inst})*(dn_{EV})^2 \quad (29)$$

where the residual offset coefficient $a_{0\_BCS}(B,T_{inst})$ and second-order $a_{2\_BCS}(B,T_{inst})$ are determined using equation (25), and the HAM side dependent linear response $b_{1\_OBC}(B,T_{inst})$ is determined on a scan-by-scan basis by

$$b_{1\_OBC}(B) = [\Delta L_{OBC}(B) - a_{0\_BCS}(B) - a_{2\_BCS}(B)*(dn_{OBC})^2]/dn_{OBC} \quad (30)$$

where $\Delta L_{OBC}(B)$ is given in equation (28) and

$$dn_{OBC} = \frac{1}{M_{OBC}} \cdot \sum_{i=1}^{M_{OBC}} DN_{OBC} - \frac{1}{M_{SVS}} \cdot \sum_{i=1}^{M_{SVS}} DN_{SVS} \quad (31)$$

OBC BB spectral radiance is too low to provide a useful signal for low gain range M13 band observation. Low gain M13 DNs will be calibrated using pre-launch coefficients that may be adjusted as needed based on vicarious calibration analysis.

During pre-launch thermal vacuum testing the VIIRS thermal model is verified and which thermistor or thermistors to use for T_{inst} are determined.

To achieve slowly varying behavior, the linear response term is averaged over previous N_{scans}.

$$\overrightarrow{b_{1\_OBC}}(B) = \frac{1}{N_{scans}} \cdot \sum_{j=\frac{-N_{scans}}{2}}^{\frac{N_{scans}}{2}} \left(b_{1\_OBC,j}\right)(B) \quad . \quad (32)$$

The VIIRS telescope takes 1.786 seconds to complete a rotation. During each scan, a new measurement of the linear response (gain) is determined according to equation (31). The drift of the gain from scan to scan is expected to be very small. This slowly varying behavior is considered by averaging the linear response term over N_{scans} as shown in equation (32).

The OBC BB is cycled to 315 K and allowed to return to the Sensor thermal ambient temperature on an approximately biweekly basis. This OBC elevated temperature operation simulates the ground calibration process from which the calibration coefficients are calculated. This cycle allows for a determination of $b_{1\_OBC\_elev}(B)$. Comparison of $b_{1\_OBC\_elev}(B)$ with $b_{1\_OBC}(B,T_{inst})$ verifies the continued stability of on-orbit operation of a_{0_BCS} and a_{2_BCS}. Vicarious calibration measurements obtained during the validation phase of the VIIRS is also used to verify the stability on-orbit operation of a_{0_BCS} and a_{2_BCS} and the performance of the OBC BB.

Using the average gain (i.e., the linear response), the dn difference $\Delta_{OBC,i}$ for a given band between the ith measurement and the average of many measurements of the OBC BB is given by:

$$\Delta_{OBC,i} = dn_{OBC,i} - \overrightarrow{dn_{OBC,i}} = dn_{OBC,i} - \frac{\Delta L_{OBC,i}\cdot(B) - A_{2\_BCS}\cdot\left(dn_{OBC,i}\right)^2 - a_{0\_BCS}}{b_{1\_OBC,i}} \tag{33}$$

Similarly, for the scan i+1

$$\Delta_{OBC,i+1} = dn_{OBC,i+1} - \overrightarrow{dn_{OBC,i+1}} = dn_{OBC,i+1} - \frac{\Delta L_{OBC,i+1}\cdot(B) - A_{2\_BCS}\cdot\left(dn_{OBC,i+1}\right)^2 - a_{0\_BCS}}{b_{1\_OBC,i+1}} \tag{34}$$

The instantaneous correction to dn_{ev} is given by adding the linearly interpolated amount, according to

$$dn_{EV,i}(t) \longrightarrow dn_{EV,i}(t) + (dn_{EV,i}(t)/dn_{OBC,i}) * [(\Delta_{OBC,i+1} - \Delta_{OBC,i}) * t/1.786 + \Delta_{OBC,i}] \tag{35}$$

where the time t is measured from the center of the ith scan measurement of the OBC BB.[4]

Generalizing equation (20), the radiance difference attributed to the Earth view path and the space view path (after reflection by the HAM) is given by

$$\Delta L_{EV} = L_{EV\_PATH} - L_{SV\_PATH} = RVS_{EV}\, L_{EV} + (RVS_{SV} - RVS_{EV})L(T_{HAM}) \tag{36}$$

and similarly from equation (25)

$$RVS_{EV}\cdot\overrightarrow{L_{EV}} + \left(RSV_{SV} - RVS_{EV}\right)\cdot\overrightarrow{L\left(T_{HAM}\right)} = a_{0\_BCS}\cdot(B) + \overrightarrow{\left[b_{1\_OBC}(B)\right]}\cdot dn_{EV} + a_{2\_BCS}(B)\cdot\left(dn_{EV}\right)^2. \tag{37}$$

where the overstrike bar over the radiance terms (not the b_i term) on the left-hand side of equation (37) indicates the appropriate RSR averaging similar to equation (22).

Solving equation (37) for the band-averaged radiance from the Earth view, before the HAM reflection, representing the desired "at aperture" radiance $\overrightarrow{\left[L_{EV}(B)\right]}$ yields

[4] Equations (33), (34), and (35) are patterned after Guenther, B. et al, (July 1998), *Prelaunch Algorithm and Data Format for the Level 1 Calibration Products for the EOS-AM1 Moderate Resolution Imaging Spectroradiometer (MODIS)*, IEEE Transactions on Geoscience and Remote Sensing, Vol. 36, No. 4, July 1998 where a running average of scans before and after the current scan is used in averaging. For VIIRS the running average will be over the past N scans.

$$\overrightarrow{\left[L_{EV}(B)\right]} = \frac{1}{RVS_{EV}(\lambda)}\cdot\left[a_{0\_BCS}(B) + \overrightarrow{b_{1\_OBC(B)}}\cdot dn_{EV} + a_{2\_BCS}(B)\cdot\left(dn_{EV}\right)^2\right]\ldots$$
$$+-\left[\frac{\left[\left(RVS_{SV}\right)(\lambda) - RVS_{EV}(\lambda)\right]}{RVS_{EV}(\lambda)}\cdot\frac{\int L\left(T_{HAM},\lambda\right)\cdot RSR(B,\lambda)\,d\lambda}{\left(\int RSR(B,\lambda)\,d\lambda\right)n}\right] \quad (38)^{5}$$

In summary, $\overrightarrow{\left[L_{EV}(B)\right]}$ is determined directly or indirectly by

$\overrightarrow{\left[L_{EV}(B)\right]}$ = L_{EV}[a_{0_BCS}(B),b_{1_OBC}, a_{2_BCS}(B), RVS_{SV}(B), RVS_{EV}(B), RVS_{OBC}(B), ε_{OBC}(B),

ΔT_{OBC}(B), RSR(B,λ) T_{OBC}, T_{HAM}, F_{sh}, F_{cav}, F_{tele}, T_{sh}, T_{cav} ,T_{tele}, T_{inst}, DN_{EV}, DN_{OBC}, DN_{SV}]

Where the coefficients a_{0_BCS}(B), a_{2_BCS}(B)), RVS_{SV}, RVS_{EV}, RVS_{OBC}, ε_{OBC}(B), F_{sh}, F_{cav}, F_{tele}, and RSR(B,λ) are determined from pre-launch characterization / calibration measurements. RVS_{SV}, RVS_{EV} and RVS_{OBC} are HAM side and spectral band dependent. RVS is not expected to vary from detector to detector in the same spectral band. The remaining parameters (T_{OBC}, T_{HAM}, T_{sh}, T_{cav}, T_{tele}, T_{inst}, DN_{EV}, DN_{OBC}, and DN_{SV}) are determined from on-orbit data / telemetry.

Gain specific correction and conversion factors are stored as LUTs for use with the dual gain M13 band. This adds a dimension to each factor and introduces the requirement on the processing software to identify and select the correct values to use for each sample.

Following radiometric calibration of the M13 band an along-scan aggregation is performed as part of the process of building the output SDR products. This aggregation is performed to exactly match the aggregation that is performed on board for the single gain bands. Calibrated TOA radiances for the unaggregated sub-pixel samples that would otherwise be discarded are saved in the Calibrated Dual Gain IP file for analysis or production of special interest products that may be desired from time to time. The Calibrated Dual Gain IP file is described in detail in the *VIIRS Radiometric Calibration Unit Level Detailed Design [Y2490]*.

[5] The Mathcad notation "+-" means "-".

3.3.3 Day/Night Band

The DNB detector is a backside-illuminated Charge-Coupled Device (CCD) with four separate light-sensitive stages having three different gains. (Duplicate copies of the most sensitive stage are provided for use in correcting radiation effects in the data.) The detector elements in the CCD are only 15.5µm (scan) x 24.2 µm (track), which is much smaller than the approximately 435µm x 1,016µm dimensions of other VIIRS detectors. During the course of the VIIRS active Earth scan, the DNB maintains an approximately constant Horizontal Sample Interval and Instantaneous Field of View on the ground by aggregating the signals from various numbers of these "sub-pixel" detectors to compensate for the variations that would otherwise occur during the scan. Thirty-two different aggregation modes are used during the scan.

Table 3 shows some design and performance characteristics of the DNB. The CCD sensor operates in a Time Delay Integration (TDI) mode, in which the accumulating photoharge is clocked through the CCD in the same direction and at the same rate that the real image of the scene is scanned across the CCD chip. Every 3.84 microseconds this process delivers a row of 672 sub-detector charge packets to the downstream end of each CCD stage. The charges from a variable number of these rows of packets are accumulated in an accumulator register, thereby effectively aggregating a variable number of sub-pixels in the scan direction. The charges are then transferred into a high-speed shift register that moves the charge in the cross-scan direction to the chip output amplifiers. A summing node just before the amplifier inputs aggregates charge in the cross-scan direction in a manner similar to along-scan aggregation. The net result is that the packets of charge delivered to the chip output amplifiers each represent the charge from N x M sub-pixels, where N and M are the number of charge packets accumulated between readouts in the two directions. As indicated in Table 3, the aggregation modes used in normal DNB operation vary from 11 vertical (i.e. along-scan) x 20 horizontal (i.e. along-track) to 66 vertical x 42 horizontal. The output amplifier produces a voltage that is (nominally) a linear function of the number of electrons delivered to its input.

Table 3. VIIRS DNB Characteristics.

	Stage 1A	Stage 1B	Stage 2	Stage 3
Subpixel Dimension - Scan (µm)	15.4	15.4	15.4	15.4
Subpixel Dimension - Track (µm)	24.2	24.2	24.2	24.2
Number of Detectors In TDI	250	250	3	1
Neutral-Density Filter	none	none	none	35 x
Min Signal Radiance (W/cm^2-sr)	3.9E-11	3.9E-11		
Max Signal Radiance (W/cm^2-sr)	3.8E-08	3.8E-08	2.3E-05	4.5E-03
Required Calibration Uncertainty (%)				
Minimum Radiance	100%	100%	30%	10%
Mid-Range Radiance				5%
Maximum Radiance	30%	30%	10%	

The CCD aggregation process described above is extremely efficient; and when the DNB is observing a uniform scene it approaches perfect efficiency. As a result it is possible to deliver to the amplifier charge packets whose relative sizes are precisely known by observing a constant uniform scene and varying the aggregation values applied. By providing an appropriate source (the on-board Solar Diffuser) and a sufficiently wide range of aggregation modes, this process is used to characterize the transimpedance (gain) of the DNB Stage 3 (high radiance range) output amplifiers.

3.3.3.1 Pre-launch Radiometric Calibration

Data are acquired from the DNB in each of its 32 aggregation modes during pre-launch testing. The SIS provides optical stimuli and the SVS provides a reference signal. The single point calibration of the mid gain and high gain stages of the DNB probably requires the addition of a calibrated neutral density filter between the standard lamp and the diffuser as well as increasing the lamp to diffuser distance, due to the low light levels involved. The full scale spectral radiance for the high gain stage is a factor of 24 lower than L_{min} of band M11, and the full scale spectral radiance for the mid gain stage is comparable to L_{min} for several of the other bands. Due to the low light levels involved, this entire test set-up must be shrouded up to the thermal vacuum chamber window, and all laboratory lighting must be "OFF".

Response Linearity of the DNB Low Gain Stage

The response linearity test is performed at each of the three temperature plateaus during the thermal vacuum test sequence. For this test the VIIRS DNB is cycled through each of its 32 aggregation modes beginning with aggregation mode 1 (66 in scan and 42 in track). The appropriate lamps are selected to provide a near full-scale signal for the DNB

Response Linearity of the DNB Mid and High Gain Stages

The linearity characterization of the mid gain and high gain stages of the DNB requires a different test set-up to attain the low light levels required.

To characterize the linearity of the two most sensitive stages of the DNB, the spectral radiance source at the focal plane of the Scattering Measurement Assembly (SCMA) is the exit port of an 8 inch (20 cm) gold coated SIS. Two entrance ports are utilized. One port houses three lamps for characterizing the mid gain stage. The characterization of the high gain stage utilizes an aperture wheel located immediately behind the second port. The rotary position of the aperture wheel is computer controlled via a stepper motor. The wheel is illuminated by a single incandescent lamp located 5 inches away. Five apertures ranging in diameter from 0.0125 inches to 1.25 inches are selectable by command. As in the testing of the other reflective bands, a mechanically actuated attenuator can be inserted into the optical path between the exit port and the SCMA mirror. This entire test set-up must be shrouded up to the thermal vacuum chamber window, and all laboratory lighting must be "OFF".

The acquisition of linearity data for the mid and high gain stages of the DNB is similar to that for the other reflective bands, except for the following:

The linearity data for the DNB is acquired for all 32 aggregation modes of the DNB beginning with aggregation Mode 1 (66 in scan and 42 in track). At three arbitrary illumination levels between L_{min} and 0.9 L_{max} of each stage, 20 (TBD) scans of data are acquired for each aggregation mode of the DNB (mode 1 through mode 32). These data are used to evaluate the Relative Response of the mid and high gain stages.

NOTE: At the end of this test, while the test set-up is intact, data for one additional test must be acquired.

A minimum of 20 scans of data must be acquired at a spectral radiance of L_{min} for the high gain stage of the DNB (7.5 E-5 W/m^2-sr-µm). These data are used in evaluating DNB SNR. These SNR data are acquired with the DNB in Aggregation Mode 32 (11 elements in scan and 20 elements in track)

Relative Response of the DNB (Low Gain Stage)

The relative response of the low gain stage of the DNB is evaluated by scanning the SIS(100) with the SIS lamps sequenced in a manner to provide three levels between L_{min} and 0.9 L_{max}.

Twenty scans (TBR) of data are acquired for each lamp level for each aggregation mode of the DNB (mode 1 through mode 32). The signal levels are equal to the difference between the DN values obtained during the active scan of the SIS and the DN values obtained while scanning the SVS. The averaged data thus acquired are "calibrated" using the radiometric transfer functions (second order polynomials) and the calibrated values for each aggregated detector of the DNB are compared to the value at L_{max} to determine compliance with DNB requirements.

Relative Response of the DNB (Mid and High Gain Stages)

The mid gain and high gain stages of the DNB are evaluated for relative radiometric response by using the data acquired in the response linearity testing. Each of the three illumination levels and each of the aggregation modes are averaged and "calibrated" using the radiometric transfer functions (second order polynomials). The calibrated values for each aggregated detector of the DNB mid and high gain stages are compared to the value at L_{max} (for that stage) to determine compliance with DNB requirements.

3.3.3.2 On-Orbit Radiometric Calibration

A complete calibration of the DNB involves calibration of four detector stages in each of 32 aggregation modes. The ratio of the lowest to the highest radiance needed is approximately 6.9 million to one. The facilities for such a calibration are difficult to provide on the ground, and are totally impractical in space. Fortunately, an adequate calibration is possible with just the single accurately known radiance provided by the VIIRS Solar Diffuser (SD), supplemented by occasional diagnostic mode observations of the Earth in the neighborhood of the terminator. In addition, observing one or more Earth scenes under very low but known illumination can check the results. On-orbit DNB calibration takes advantage of a VIIRS diagnostic capability to transmit both the highest and lowest-radiance VIIRS stages simultaneously with the composite DNB data when the Earth is being observed.

The minimum available signal into the amplifiers is determined by the minimum radiance of the SD at the minimum aggregation mode. At the time of this writing the SD design was not final, but its minimum radiance is expected to be approximately equivalent to a 3% Earth albedo.

Since the expected signal range into the DNB extends to 100% albedo at maximum aggregation, this minimum calibrator signal corresponds to roughly 0.24% of the maximum signal. With the CCD in its largest normal aggregation mode the signal is still only 3% of the maximum. However, for test purposes the CCD can be operated with aggregation in the scan direction of up to 1,023 sub-pixels. This provides 46% of the maximum expected signal to the amplifier. This is larger than the signal due to a 100% albedo scene in most aggregation modes. At other times of year the Sun angle on the SD results in a signal equivalent to roughly 7% Earth albedo. At these times, the aggregation range allows calibration of the amplifiers up to their maximum expected signals.

This process provides in-flight calibration of the high-range output amplifiers over essentially their entire anticipated operating range. The accuracy of the calibration is limited by the uncertainty in knowledge of the SD radiance and by the response non-uniformity of the sub-pixel detectors. (CCD Charge Transfer Inefficiency is a second-order effect that essentially disappears for uniform scenes such as the calibrator.) Initial images made by the first DNB CCDs have exhibited excellent response uniformity even at the sub-pixel level. Moreover the aggregation process reduces whatever non-uniformity is present by the square root of the number of detectors aggregated in the cross-scan direction. If the sub-pixels had an RMS non-uniformity of 5%, this would result in non-uniformity of only 0.7% to 1.1% in the aggregated pixels, depending on the aggregation mode. These numbers can be further reduced by the square root of 8 because each output amplifier processes 8 uncorrelated pixels.

One of the primary effects of radiation on orbit is expected to be degradation in sub-pixel response uniformity. Recent radiation tests provide data indicating the magnitude of any degradation. In addition, the impact of non-uniformity on the aggregated pixels are directly measurable in the observations of the SD. These data can be used along with accumulated Earth data statistics to develop the equations for “de-striping” the DNB Earth image data.

The Solar Diffuser calibration described above measures the linearity and radiometric performance of DNB Stage 3, the highest-radiance, lowest gain stage. It is also necessary to determine the radiometric gains of the higher-gain DNB stages, although the required calibration accuracy for these stages is significantly looser.

To calibrate the more sensitive DNB stages, data collected from Earth scenes are used to determine the relative gain between the stages. To do this accurately it is necessary to collect and transmit the data from two adjacent CCD gain stages simultaneously from the same location on the Earth under the same viewing conditions. Further, the radiance of the data collected must be in the relatively narrow overlap region where the data collected from both gain stages is within their useful dynamic range. Fortunately, radiances corresponding both to the Stage 1-Stage 2 overlap and the Stage 2-Stage 3 overlap occur in the neighborhood of the terminator. The radiances are thus visible twice each orbit for non-terminator orbiting Sensors, and almost continuously for terminator-orbiting Sensors.

The necessary ‘calibration’ data can be collected by simultaneously transmitting data from the moderate-gain and high-gain DNB CCD stages while the normal “piecewise-linear” DNB data processing continues to operate. Since the scene radiance increases (or decreases) as the Sensor flies over the terminator, at some point the Earth scene radiance crosses through each of the two "crossover" regions where the radiance is within the useful range of two DNB stages. Similarly, for a Sensor in a terminator orbit (i.e. the 17:30 local equator crossing time orbit), the two "crossover" regions exist at different points in the same scan.

The extra two stages of DNB CCD data are transmitted only for a few minutes or less on rare occasions. At these times VIIRS is placed in Diagnostic Mode and the data from DNB Stage 1A or 1B (as commanded) replaces the data from Band M1, while the data from DNB Stage 2 replaces the data from Band M2. These calibrations can be performed at times in the orbit when Bands M1 and M2 are not contributing to useful EDR production.

A check of the radiance calibration for the most sensitive DNB stages is made based on observation of selected Earth regions where brightness under lunar illumination is well known. Candidate areas include White Sands, NM, the Bonneville Salt Flats, UT, and locations in the deserts of the Middle East. Under full moon illumination these regions generally provide at least five times the minimum specified radiance of the DNB.

As computed the DNB calibrated TOA radiances are spectral radiance in W/m^2-sr-μm (as is the case with other bands). However users of this product prefer integrated radiance in W/cm^2-sr. Therefore a conversion to W/cm^2-sr is performed prior to storing in the DNB SDR files. The correction factor is determined from each Sensor's DNB spectral response function and is stored in the DNB LUT.

3.4 PRACTICAL CONSIDERATIONS

3.4.1 Numerical Computation Considerations

Paragraph SRDV3.2.1.5.4-1 of the VIIRS SRD states the following:

> "*The scientific SDR and EDR algorithms delivered by the VIIRS contractor shall be convertible into operational code that is compatible with a 20 minute maximum processing time at either the DoD Centrals or DoD field terminals for the conversion of all pertinent RDRs into all required EDRs for the site or terminal, including those based wholly or in part on data from other sensor suites*."

This essentially means that any and all EDRs must be completely processed from VIIRS raw data, including calibration and georeferencing within 20 minutes from the time the raw data are available. This requirement is a strong reminder that VIIRS is an operational instrument.

The complexity of the calculations used for VIIRS radiometric calibration is similar to those in routine MODIS processing and are therefore expected to perform within a reasonable allocation of the operational timeline. Furthermore the calculations to convert calibrated TOA reflectances to calibrated TOA radiances and from calibrated TOA radiances to calibrated TOA brightness temperatures are straightforward and leave minimal additional impact on VIIRS processing resources.

3.4.2 Programming and Procedural Considerations

It is expected that some adjustments will have to be made to the calibration coefficients and/or radiance/reflectance values to account for on-orbit changes in instrument characterization and to account for small differences in individual detector throughput and the optical characteristics of the two sides of the VIIRS HAM. The nature of these adjustments may not be known before the VIIRS Radiometric Calibration software is complete. Therefore, through the use of external band-detector-HAM side LUTs, the VIIRS software architecture has been designed to be flexible enough to accommodate adjustments if and when needed.

Details of the software for radiometric calibration are presented in the *VIIRS Context Software Architecture [Y2469]*, the *VIIRS Build SDR Module Level Software Architecture [Y2479]*, and the *VIIRS Radiometric Calibration Unit Level Detailed Design [Y2490]*. The efficient storage of the SDR products is detailed in *[Y2490]*.

3.4.2.1 Quality Control

The VIIRS radiometric calibration algorithm includes many checks on the reasonableness of input data and output product. The quality bit assigned to each pixel's calibrated TOA radiance, TOA reflectance, and TOA brightness temperature is set should some problem be detected during radiometric calibration. This quality bit serves as a flag to the subsequent EDR generation algorithms to avoid using such a pixel.

3.4.2.2 Exception Handling

Warning and error messages that may be issued during radiometric calibration are stored in a log file and appropriate return codes are set to control program action and to communicate status to system process control software. Details of exception handling are in the *VIIRS Radiometric Calibration Unit Level Detailed Design [Y2490]*.

3.4.3 Initialization

Initialization is accomplished by populating the reflective, emissive, and DNB LUTs. Prior to launch of each Sensor these LUTs are constructed using the best available analysis results from pre-launch sensor testing.

4.0 ASSUMPTIONS AND LIMITATIONS

4.1 ONBOARD PROCESSING

It is assumed that onboard processing aggregates the imagery resolution and single gain moderate resolution band DNs as is described in Section 2.2.3. Furthermore it is assumed that the DNB operates and the onboard data processing is performed according to the *DNB CCA Product Specification for VIIRS [PS154640-380]*, the *DNB Module Performance Specification NPOESS [PS154640-124]*, and the *Digital Preprocessor Product Specification for VIIRS [PS154640-360]*.

4.2 INPUT DATA

It is assumed that the reflective band, emissive band, and DNB LUTs are populated with complete and correct calibration parameters. It is assumed that the Verified VIIRS RDR input is as described in the *VIIRS Build RDR Module Level Detailed Design [Y2487]* and that geolocation data are available as described in the *VIIRS Geolocation Unit Level Detailed Design [Y3245]*.

4.3 PRE-LAUNCH CALIBRATION

It is assumed that pre-launch calibration for each Sensor is adequate to characterize the Sensor and provide the data needed for the reflective, emissive, and DNB radiometric calibration LUTs.

5.0 REFERENCES

5.1 VIIRS DOCUMENTS

The following VIIRS documents are referenced in this ATBD using their Raytheon SBRS document number in italicized brackets, e.g., *[Y12345]*:

[PS154640-102]	Performance Specification Algorithm Specification for the VIIRS
[PS154640-124]	DNB Module Performance Specification NPOESS
[PS154640-360]	Digital Preprocessor Product Specification for VIIRS
[PS154640-380]	DNB CCA Product Specification for VIIRS
[TP154640-001]	VIIRS System Verification and Validation Plan
[TP154640-118]	VIIRS Characterization and Calibration Plan
[Y2388]	VIIRS Software Development Plan
[Y2469]	VIIRS Context Software Architecture
[Y2470]	VIIRS Data Interface Control Document
[Y2479]	VIIRS Build SDR Module Level Software Architecture
[Y2487]	VIIRS Build RDR Module Level Detailed Design
[Y2490]	VIIRS Radiometric Calibration Unit Level Detailed Design
[Y3245]	VIIRS Geolocation Unit Level Detailed Design
[Y3258]	VIIRS Geoocation ATBD
[Y5235]	Methodology to characterize VIIRS non-linearity - micro and macro
[Y5563]	Closure Memo for VIIRS PDR Action Items 29, 43, 47, and 78
[Y6875]	Terminator Orbit Calibration
[Y0012275]	Description of DC Restore Process in the VIIRS Sensor
[Y0012416]	VIIRS Cross-Calibration Method for Terminator Orbit Sensors

5.2 NON-VIIRS DOCUMENTS

The following non-VIIRS documents are references for this ATBD:

1. Barnes, W.L., Thomas S. Pagano, and Vincent V. Salomonson, (July 1998), *Prelaunch Characteristics of the Moderate Resolution Imaging Spectroradiometer (MODIS) on EOS-AM1*, IEEE Transactions on Geoscience and Remote Sensing, Vol. 36, No. 4, July 1998. 13 pp.

2. Che, N., B. G. Grant, D. E. Flittner, P. N. Slater, and S. F. Biggar, *Results of Calibrations of the NOAA-11 AVHRR made by reference to calibrated SPOT imagery at White Sands, N.M.*, Proc. SPIE Vol. 1943-21, 1991.

3. Guenther, B. et al, (July 1998), *Prelaunch Algorithm and Data Format for the Level 1 Calibration Products for the EOS-AM1 Moderate Resolution Imaging Spectroradiometer (MODIS)*, IEEE Transactions on Geoscience and Remote Sensing, Vol. 36, No. 4, July 1998. 10 pp.

4. IPO (2000). *Visible/Infrared Imager/Radiometer Suite (VIIRS) Sensor Requirements Document (SRD) for National Polar-Orbiting Operational Environmental Satellite System (NPOESS) Spacecraft and Sensors*, Rev. 2b/c. Prepared by Assoc. Directorate for Acquisition, NPOESS Integrated Program Office, Silver Spring, MD.

5. MODIS Characterization Support Team (May 1997). *MODIS Level 1B Algorithm Theoretical Basis Document Version 2.0*, MCST Document #MCM-ATBD-01-U-DNCN, NASA/GSFC, Greenbelt, MD.

6. MODIS Characterization Support Team (2000). *MODIS Level 1B Product User's Guide, For Level 1B Version 2.3.x*, Release 2, MCST Document #MCM-PUG-01-U-DNCN, NASA/GSFC, Greenbelt, MD.

7. Planet, W.G. (ed.), (1988). *Data Extraction and Calibration of TIROS-N/NOAA Radiometers*. NOAA Technical Memorandum NESS 107 – Rev. 1, Oct. 1988. 130 pp.

8. Scott, K. P., *Radiometric Calibration of On-Orbit Satellite Sensors Using an Improved Cross-Calibration Method*, Ph.D. Dissertation, Univ. of Arizona, 1998.

9. Scott, K. P., K. J. Thome, and M. R. Brownlee, *Evaluation of the Railroad Valley playa for use in vicarious calibration*, Proc. SPIE Vol. 2818, 1996.

10. Teillet, P. M., P. N. Slater, Y. Ding, R. P. Santer, R. D. Jackson, and M. S. Moran, *Three methods for the absolute calibration of the NOAA AVHRR sensors in-flight*, Remote Sens. Environ., 31:105-120, 1990.